N O T I C E

THIS DOCUMENT HAS BEEN REPRODUCED FROM MICROFICHE. ALTHOUGH IT IS RECOGNIZED THAT CERTAIN PORTIONS ARE ILLEGIBLE, IT IS BEING RELEASED IN THE INTEREST OF MAKING AVAILABLE AS MUCH INFORMATION AS POSSIBLE

NASA TECHNICAL MEMORANDUM

NASA TM-75806

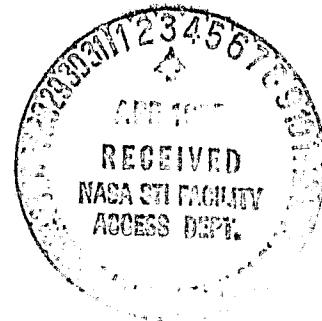OUTLINE OF RESEARCH ON OSCILLATING BOUNDARY LAYERS

J. Cousteix

Translation of "Apercu General Des Recherches Sur Les Couches
Limites en Ecoulement Pulse," 15th Colloquium on Applied
Aerodynamics, Marseille, 7-9 November 1978, pp. 1-22

NATIONAL AERONAUTICS AND SPACE ADMINISTRATION
WASHINGTON, D.C. 20546   NOVEMBER 1979

1. Report No. NASA TM-75806	2. Government Accession No.	3. Recipient's Catalog No.
4. Title and Subtitle OUTLINE OF RESEARCH ON OSCILLATING BOUNDARY LAYERS		5. Report Date November 1979
		6. Performing Organization Code
7. Author(s) J. Cousteix, National Office of Aerospace Study and Research (ONERA), CERT, Toulouse, France		8. Performing Organization Report No.
		10. Work Unit No.
9. Performing Organization Name and Address Leo Kanner Associates Redwood City, California 94063		11. Contract or Grant No. NASw-3199
		13. Type of Report and Period Covered Translation
12. Sponsoring Agency Name and Address National Aeronautics and Space Administration, Washington, D.C. 20546		14. Sponsoring Agency Code

15. Supplementary Notes

Translation of "Apercu General Des Recherches Sur Les Couches Limites en Ecoulement Pulse." 15th Colloquium on Applied Aerodynamics, Marseille, 7-9 November 1978, pp. 1-22 (A79-32279)

16. Abstract

An outline of the state of the art in the field of unsteady boundary layers is given. From a practical point of view, turbulent boundary layers are of particular interest. Very recent experimental and theoretical progress achieved is emphasized. The unsteady flows considered are mainly periodic flows on the average, with the external velocity varying around a zero or nonzero mean time value. However, for a good understanding of certain unsteady phenomena, the principal results obtained on laminar boundary layers are given.

17. Key Words (Selected by Author(s))	18. Distribution Statement
	Unclassified-Unlimited

19. Security Classif. (of this report) Unclassified	20. Security Classif. (of this page) Unclassified	21. No. of Pages 51	22. Price

OUTLINE OF RESEARCH ON OSCILLATING BOUNDARY LAYERS

J. Cousteix
National Office of Aerospace Study and Research
(ONERA), CERT, Toulouse, France

1. Introduction

Very diverse motives associated with the subjects of research   /1*
and application in fields, such as aerodynamics, hydrodynamics, bio-
mechanics, meteorology and oceanography, have stimulated study of un-
steady flows.

We are particularly interested in the behavior of turbulent unsteady
boundary layers in aeronautics, especially in helicopter and jet engine
problems. The turbulence parameter is of fundamental interest in this
limited field of unsteady aerodynamics. In fact, it appears that the
analysis of unsteady flows can contribute interesting data for model-
ing and calculation of turbulent flows.

The most common unsteady flows are periodic and, quite naturally,
they are associated with the basic case of oscillatory flow. We review
recent work on this question, limited to that on the boundary layer.
Other fundamental subjects, such as wakes, jets and flows in ducts, are
being studied in several laboratories and also are very important, but
they are set aside from this review.

Except for the work of Karlsson, it can be said that the development
of calculation methods preceded that of experiments. This is partially
explained by the necessity of having available means of acquisition of
numerical data, while most of the means used so far have been analogic,
this need being connected with the need of special statistical analysis
of experimental data. Several experiments actually have been conducted,
others are in progress, and they permit specification of the description
of unsteady effects. They also permit a little broader discussion of
the validity of available calculation methods.

---

*Numbers in the margin indicate pagination in the foreign text.

Before describing these studies, we think it useful to recall some results on laminar boundary layers, which assist in understanding some aspects of the unsteadiness of the flow.

2. Laminar Flow

While the equations of unsteady laminary boundary layers are known with great certainty, the understanding and analysis of some questions have only recently been elucidated, in particular, by the use of asymptotic expansion methods.

The best known flows are oscillating flows, in which the average velocity can be zero or nonzero. Before describing the main results for these flows, it is advisable to stress some precautions to be taken, before using the classical boundary layer equations.

2.1. Boundary Layer Equations (Incompressible)

The Navier-Stokes equations quite clearly are the fundamental equations. In everything which follows, we are intested mainly in incompressible flows, and this restriction implies conditions [Lighthill, 43, 44]. In isothermal flow, the two principal conditions are: 1. Mach number a little less than one; 2. the acoustical wavelength associated with characteristic frequency ω should be large, with respect to characteristic dimension L of the system. With v as the characteristic velocity and c, the speed of sound, these conditions are described by

$$v/c \ll 1 \qquad \omega L/c \ll 1$$

In this case, the fundamental equations are:

$$\frac{\partial u_i}{\partial x_i} = 0 \tag{1}$$

$$\frac{\partial u_i}{\partial t} + u_j \frac{\partial u_i}{\partial x_j} = -\frac{1}{\rho} \frac{\partial p}{\partial x_i} + \nu \frac{\partial^2 u_i}{\partial x_\ell^2} \tag{2}$$

2

Discussion of the validity of the classical boundary layer equations, namely,

$$\frac{\partial u}{\partial x} + \frac{\partial v}{\partial y} = 0 \tag{3}$$

$$\frac{\partial u}{\partial t} + u\frac{\partial u}{\partial x} + v\frac{\partial u}{\partial y} = -\frac{1}{\rho}\frac{\partial p}{\partial x} + \nu\frac{\partial^2 U}{\partial y^2} \tag{4}$$

$$\frac{\partial p}{\partial y} = 0 \tag{5}$$

often brings numerous parameters into play in the unsteady case. We illustrate this with the simple case of a body of characteristic dimension L, located in a fluid oscillating at frequency ω. U_0 is a typical magnitude of the amplitude of the velocity variation, and we shall see that the order of magnitude of the thickness of the viscous layer is $(\nu/\omega)^{1/2}$. It uses a system of axes connected to the wall, and it introduces the following dimensionless quantities:

$$Y = y/(\nu/\omega)^{1/2} \qquad T = \omega t \qquad X = x/L$$

$$U = u/U_0 \qquad V = v(\omega L^2/\nu)^{1/2}/U_0 \qquad P = p/\rho\omega U_0 L$$

Disregarding all effects of curvature, the two dimensional Navier-Stokes equations become

$$\frac{\partial U}{\partial X} + \frac{\partial Y}{\partial Y} = 0 \tag{6}$$

$$\frac{\partial U}{\partial t} + \frac{U_0}{\omega L}\left(U\frac{\partial U}{\partial X} + V\frac{\partial U}{\partial y}\right) = -\frac{\partial P}{\partial X} + \frac{\nu}{\omega L^2}\frac{\partial^2 U}{\partial X^2} + \frac{\partial^2 U}{\partial y^2} \tag{7}$$

$$\frac{\partial V}{\partial t} + \frac{U_0}{\omega L}\left(U\frac{\partial V}{\partial X} + V\frac{\partial V}{\partial y}\right) = -\frac{\omega L^2}{\nu}\frac{\partial P}{\partial y} + \frac{\nu}{\omega L^2}\frac{\partial^2 V}{\partial X^2} + \frac{\partial^2 V}{\partial y^2} \tag{8}$$

It then is clear that the solution of the problem brings into play two parameters: the Strouhal number $\omega L/U_0$ and the frequency parameter $\omega L^2/\nu$. In particular, it is noted that, if $\omega L^2/\nu$ is not large enough, $\frac{\partial^2 U}{\partial x^2}$ term (Eq. 7) can be nonnegligible, and the classical boundary layer equations are no longer applicable.

3

In some cases, only longitudinal length L is not sufficient to characterize the problem. For example, if the flow is perturbed by a progressive wave, the phase velocity of which is Q, it is seen that discussion of the validity of the boundary layer equations brings in the ratio of the wavelength Q/ω to the thickness δ of the boundary layer.

Therefore, by means of these examples, it is seen that the Reynolds number is not, as it often is the steady state case, the determining parameter, and that each problem requires detailed determination of the orders of magnitude of the various terms which appear in the equations.

2.2. Oscillation with Zero Average Flow

2.2.1. Stokes Solution

The simplest case of an unsteady boundary layer is that of a parallel flow (v = 0) oscillating around an average zero. Besides, it concerns an exact solution of the Navier-Stokes equations, which is reduced simply to

$$\frac{\partial u}{\partial t} = \frac{\partial U_e}{\partial t} + \nu \frac{\partial^2 U}{\partial y^2} \tag{9}$$

With the conditions at the limits,

$$u = 0 \qquad y = 0$$
$$u \longrightarrow U_e = U_{1_e} \cos \omega t \qquad y \longrightarrow \infty$$
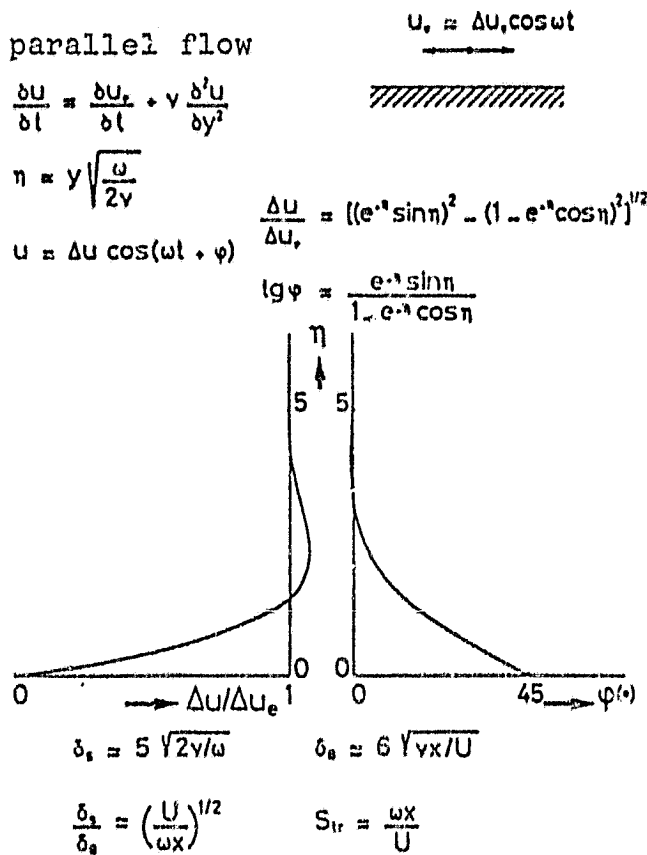
The solution found, as a function of reduced variable $\tilde{y} = y(\omega/2\nu)^{1/2}$, is written

$$\frac{U}{U_{1e}} = \cos \omega t - e^{-\tilde{y}} \cos (\omega t - \tilde{y})$$

$$\text{or } \frac{U}{U_{1e}} = \frac{U_1}{U_{1e}} \cos (\omega t + \varphi) \tag{10}$$

with

$$\frac{U_1}{U_{1e}} = \left(1 - 2 e^{-\tilde{y}} \cos \tilde{y} + e^{-2\tilde{y}} \right)^{1/2}$$

$$tg\,\varphi = \frac{e^{-\tilde{y}} \sin \tilde{y}}{1 - e^{-\tilde{y}} \cos \tilde{y}}$$

4

The reduced amplitude U_1/U_{1e} and phase ϕ profiles are presented in Fig. 1. An excess of amplitude in the boundary layer, with respect to the exterior, is noted. A large phase shift also is noted near the wall. At $y = 0$, the limiting velocity, i.e., also friction, is before $\pi/4$.

parallel flow

$$u_* = \Delta u_* \cos \omega t$$

$$\frac{\delta u}{\delta t} = \frac{\delta u_*}{\delta t} + \nu \frac{\delta^2 u}{\delta y^2}$$

$$\eta = y\sqrt{\frac{\omega}{2\nu}}$$

$$u = \Delta u \cos(\omega t + \phi)$$

$$\frac{\Delta u}{\Delta u_*} = [(e^{-\eta}\sin\eta)^2 - (1 - e^{-\eta}\cos\eta)^2]^{1/2}$$

$$\lg\phi = \frac{e^{-\eta}\sin\eta}{1 - e^{-\eta}\cos\eta}$$

$$\delta_* = 5\sqrt{2\nu/\omega} \qquad \delta_8 = 6\sqrt{\nu x/U}$$

$$\frac{\delta_*}{\delta_8} = \left(\frac{U}{\omega x}\right)^{1/2} \qquad S_{tr} = \frac{\omega x}{U}$$

Fig. 1. Stokes problem.

Practically, it can be considered that the thickness of the Stokes layer, is on the order of $5(2\nu/\omega)^{1/2}$. When the frequency increases, the unsteady effects due to viscosity are confined to a thinner and thinner layer.

This problem can be considered in a slightly different manner, by finding the perturbation produced by an infinite oscillating plate in a flow at rest. Then, the conditions at the limit are

$$U = U_{1p}\cos\omega t \qquad y = 0$$
$$u \longrightarrow U_e = 0 \qquad y \longrightarrow \infty$$

and the solution is written

$$\frac{U}{U_{1p}} = e^{-\tilde{y}}\cos(\omega t - \tilde{y})$$

Thus, the oscillation of the plate creates a wave in the flow which vanishes at infinity, the phase velocity of which is $(2\omega\nu)^{1/2}$.

2.2.2. Secondary Flow Induced by Oscillating Movement (Steady Streaming)

When a body oscillates around a fixed position in a fluid at rest, it creates a secondary, stationary flow.

Stuart has studied this problem in a reference system connected to the wall. The external velocity is in the form

$$U_e = \frac{1}{2} U_0(x) \left(e^{i\omega t} + e^{-i\omega t} \right)$$

The shear layer which develops at the wall is analogous to a Stokes layer, and it can be studied by means of the following reduced variables

$$U = U_\infty V \qquad x = \mathcal{G} L \qquad y = \tilde{y} \left(2\nu/\omega \right)^{1/2}$$

$$\psi = \left(2\nu/\omega \right)^{1/2} U_\infty \chi \quad (\psi \text{ is the current function}).$$

If $\omega L^2/\nu$ is large, the solution is calculated by means of the classical boundary layer equations.

The dimensionless equations bring out the Strouhal number $S = \omega L/v$ and, if this number is very large, the solution is found, by means of an expansion, as a function of the powers of its inverse $\alpha = S^{-1}$ [43, 44]:

$$\chi = \frac{1}{2} V_0 \left(\chi_0(\tilde{y}) e^{i\omega t} + \bar{\chi}_0(\tilde{y}) e^{-i\omega t} \right)$$

$$+ \alpha \left[\chi_s(\mathcal{G}, \tilde{y}) + \frac{1}{2} \left(\chi_2 e^{2i\omega t} + \bar{\chi}_2 e^{-2i\omega t} \right) \right] + O(\alpha^2) \tag{11}$$

In the 0 order, the solution is classical. It is that of Stokes:

$$\frac{\partial \chi_0}{\partial \tilde{y}} = 1 - e^{-(1+i)\tilde{y}} \tag{12}$$

In order α, the solution is more noteworthy, for stationary component χ_s is not zero:

$$\frac{\partial \chi_s}{\partial \tilde{y}} = V_0 \frac{\partial V_0}{\partial \mathcal{G}} \left[-\frac{3}{4} + \frac{1}{4} e^{-2\tilde{y}} + 2 e^{-\tilde{y}} \sin \tilde{y} \right.$$

$$\left. + \frac{1}{4} e^{-\tilde{y}} \cos \tilde{y} - \frac{1}{2} \tilde{y} e^{-\tilde{y}} \left(\cos \tilde{y} - \sin \tilde{y} \right) \right] \tag{13}$$

This secondary stationary movement is induced by nonlinear effects, due to the convection terms of the equation of motion.

In order α, these terms bring out quadratic quantities, such as $\sin^2 \omega t$, the time average of which is not zero and which necessarily gives rise to a stationary velocity.

6

It is noted that the velocity induced at the boundary of the Stokes layer ($\tilde{y} \to \infty$) is nonzero. It is

$$U_S = -\frac{3}{4\omega} \, U_0 \, \frac{\partial U_0}{\partial x} \tag{13'}$$

Thus, the problem is to determine how the average velocity becomes zero on the exterior of the Stokes layer. Two cases are distinguished, according to the order of magnitude of the Reynolds number $R_S = U_0^2/\omega\nu$ (this Reynolds number is made up of the order of magnitude of U_S given by formula 13', $U_S \sim U_0^2/\omega L$ and of the characteristic length L).

If $R_S \gg 1$ (Fig. 2), a boundary layer, in the very classical sense of the term, develops below the Stokes layer, and its thickness δ_S is on the order of $L / \ell_S^{1/2} = L(\omega\nu)^{1/2}/U\infty$. The ratio of δ_S to thickness $\delta_S \sim (\nu/\omega)^{1/2}$ of the Stokes layer is on the order of $\frac{L(\omega\nu)_2/(\nu/\omega)^{1/2}}{U\infty} = \omega L/U_\infty = S$. It is very much greater than 1. If R_S is on the order of 1 or less than 1, the external layer is of a different nature. It should be studied, by using the linear Stokes equations of slow movement.

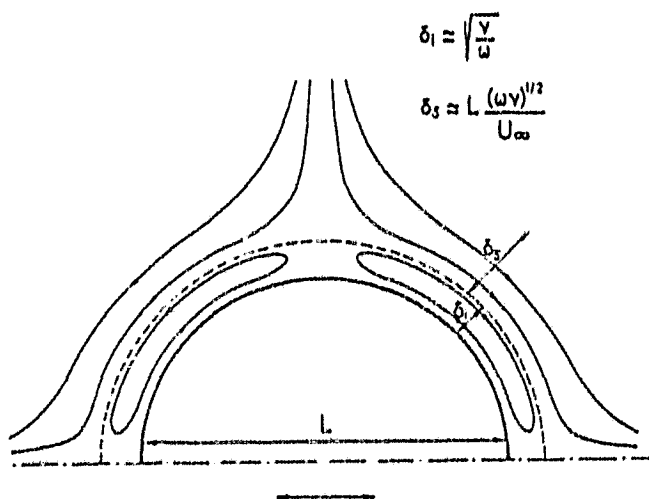$\delta_l \simeq \sqrt{\frac{\nu}{\omega}}$

$\delta_S \simeq L \frac{(\omega\nu)^{1/2}}{U_\infty}$

Fig. 2. Oscillating circular cylinder.

2.3. Oscillation with Nonzero Average Flow.

When the boundary layer develops in the presence of an external flow oscillating around an average nonzero U_0, two solutions play a fundamental part: the Blasius solution and the Stokes solution (Fig. 3). If the thicknesses of these two layers are of the same order of magnitude, the Stokes layer is fused into the stationary layer, but, if the thickness of the Stokes layer is much less, it preserves its individual nature. Now, the thickness ratio of these two layers is

$$\frac{\delta_s}{\delta_B} \sim \left(\frac{\nu}{\omega}\right)^{1/2} x \frac{(U_0 L/\nu)^{1/2}}{L} \approx \frac{1}{(\omega L/\nu)^{1/2}} = S^{-1/2}$$

The order of magnitude of the Strouhal number, therefore, is a fundamental parameter in definition of the structure of the boundary layer in such a case.

Fig. 3. Oscillating flow on flat plate (laminar).
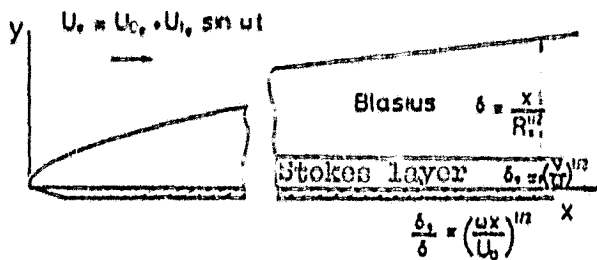
The analytical solutions of /4 this problem generally have been found, on the assumption that the external velocity fluctuation is small

$$U_e = U_{o_e}(1 + \varepsilon e^{i\omega t}) \quad \text{with} \quad \varepsilon \ll 1 \tag{14}$$

The conditions at the limits are:

$$u = v = 0 \qquad y = 0 \qquad x > 0$$
$$u \rightarrow U_e \qquad y = \infty$$
$$u = U_e \qquad x = 0 \qquad y > 0$$

The solution was found [Lighthill, 37], by expanding the velocity by powers of ε. By introducing the reduced variables

$$\tilde{t} = \omega t \qquad \tilde{x} = \omega x / U_{o_e} \qquad \tilde{y} = y(\omega/\nu)^{1/2}$$

and the reduced current function

$$\tilde{\psi} = (\omega/\nu U_{o_e}^2)^{1/2} \psi$$

the first order solution has the form

$$\tilde{\psi} = (2\tilde{x})^{1/2}(F + \varepsilon e^{i\tilde{t}} f) \tag{15}$$

If the Reynolds number $U_0 x/\nu$ is large enough, solution F is the Blasius function F_b a function^e of $\eta = \dfrac{U_0}{x}\left(\dfrac{U_{o_e} x}{2\nu}\right)^{1/2}$ alone.

In order ε, solution f can be determined numerically, whatever the reduced frequency $\tilde{x}$ [45-48]. However, analytical solutions are available

for extreme values of $\tilde{x}$.

When $\tilde{x}$ is small, f is expanded by the powers of $\tilde{x}$. The solution has the form

$$f = \sum_{n=0} (2 i \, \tilde{x})^n f_n (\eta) \tag{16}$$

where f_n is the solution of a differential equation which uses f_{n-1}.

For n=0, a quasistationary boundary solution is obtained ($\tilde{x} \to c$). f_0 is obtained by writing that Blasius function F_b is the solution at each instant. The utilization of expression (14) for U_e and expansion by a small perturbation results in

$$F_b\left(\frac{y}{x}\left(\frac{U_e x}{2 \nu}\right)^{1/2}\right) = F_b\left(\frac{y}{x}\left(\frac{U_\infty x}{2 \nu}\right)\right) + \varepsilon e^{it} \frac{\eta}{2} \frac{df_0}{d\eta} \tag{17}$$

therefore,

$$f_0 = \frac{\eta}{2} \frac{dF_b}{d\eta}$$

When the Strouhal number is large, the boundary layer has a two layer structure. Near the wall, a shear layer of the Stokes layer type develops. Its thickness is on the order of $(\nu/\omega)^{1/2}$. This internal solution is a function of $\tilde{y} = y(\omega/\nu)^{1/2}$, and it is written

$$f = \left[\tilde{y} + (1-i)(\exp(-(1+i)\tilde{y}/\sqrt{2}) - 1)\right]/(2\tilde{x})^{1/2} + O(\tilde{x}^{-1}) \tag{18}$$

The principal term is the Stokes solution.

The external layer has a thickness on the order of $x/(U_e x/\nu)^{1/2}$, and its solution is found, as a function of $\eta = \frac{y}{x}\left(\frac{U_e x}{2 \nu}\right)^{1/2}$.
It is written

$$f = \eta - (1-i)/(2\tilde{x})^{1/2} + i (F - \eta F')/2\tilde{x} + O(\tilde{x}^{-1/2}) \tag{19}$$

Figs. 4 and 5 give some summary results. Evolution of the depth of displacement and wall friction and solutions for intermediate values of the Strouhal number have been obtained numerically [45-47]. In particular, it is noted that the phase of the coefficient of friction
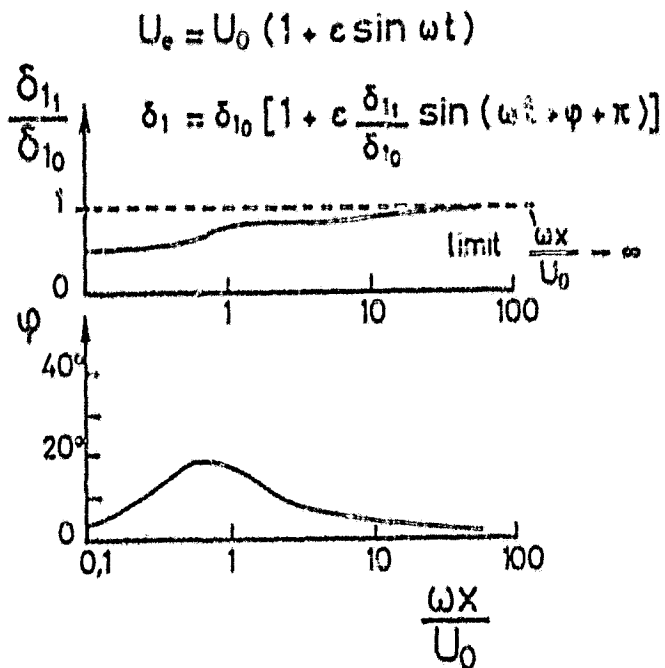
9

$$U_e = U_0 (1 + \varepsilon \sin \omega t)$$

$$\frac{\delta_{1_1}}{\delta_{1_0}} \qquad \delta_1 = \delta_{1_0} \left[1 + \varepsilon \frac{\delta_{1_1}}{\delta_{1_0}} \sin (\omega t + \varphi + \pi) \right]$$

Fig. 4. Oscillating flow on flat plate (laminar); amplitude and phase of δ_1 (from [29]).

tends toward $45°$, while x/U_{0_e} tends towards infinity, as in the Stokes solution. It also is noted that, when the Strouhal is large, the external region of the boundary layer is subjected to pulsation as a unit, when the Stokes layer is very thin. Solution (19), in fact, shows that, in this area, there is

$$U_e = U_{0_e} + \varepsilon U_{0_e} \sin \omega t$$
$$U = U_0 + \varepsilon U_{1_e} \sin \omega t$$

Consequently, product $\delta_1 U_e = \int_0^\infty (U_e - U) dy$ remains constant over time, for the very small region in the vicinity of the wall contributes little to δ_1. This explains the behavior of the amplitude and phase of δ_1 for large values of $\omega x/U_{0_e}$.

In order ε^2, a stationary term μ_s appears in the solution. If /5 numbers $R_s = (\nu \omega/U_0^2)^{1/2}$ and $\varepsilon^2 R_0 = \varepsilon^2 U_0 L/\nu$ are close to one, the boundary layer equations are applicable to calculation of μ_s [45-47]. With available experimental and numerical results taken into account, it appears that these secondary velocities are small, even for large amplitude external velocities. If this so, an important simplification results, since the average profile is the classical solution of the stationary equations. Sometimes, with an average pressure gradient, especially in the vicinity of the separation, the secondary velocities can become important.

2.4. Effect of Phase Velocity

The response of the boundary layer to a perturbation in the form

$$U_e = U_{0_e} + U_{1_e} \sin \omega \left(t - \frac{x}{Q} \right) \tag{20}$$

10

$$U_e = U_0 (1 + c \sin \omega t)$$

$$\tau_p = \tau_0 \left[1 + c \frac{\tau_1}{\tau_0} \sin(\omega t + \Phi) \right]$$
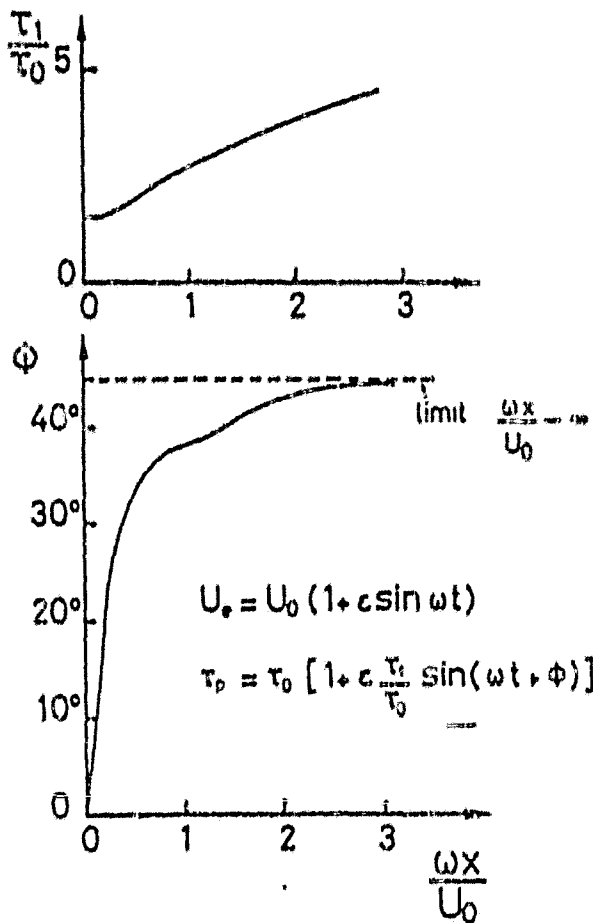
Fig. 5. Oscillating flow on flat plate (laminar); amplitude and phase of wall friction (from [29, 45-47]).

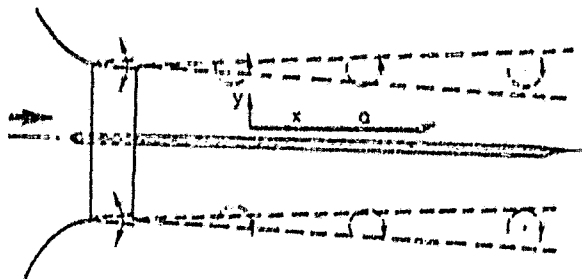
Fig. 6. Experimental assembly used by M.H. Patel; the laminar boundary layer was studied on auxiliary plate a.

depends greatly on the speed of convection of the wave Q. M.H. Patel has done an experimental study, by producing a system of eddies escaping from a swinging shutter (Fig. 6). Located in the flow at velocity U_0, the eddies move by convection at velocity Q= 0.77 U_0.

In the first order, the response of the boundary layer to the perturbation is in the form

$$U = U_0 + U_1 \sin\left(\omega (t - \frac{x}{Q}) + \varphi \right) \quad (21)$$

The experimental results indicate that the profile of continuous component U_0/U_{0_e} is not affected by the oscillation. It remains a Blasius profile (U_{0_e} is independent of x). Actually, even if there were nonlinear effects, they would be very weak, for the reduced amplitude is 10% at most.

The U_1/U_{1_e} amplitude and phase ϕ profiles have some peculiarities, especially around Strouhal numbers $\omega x/U_{0_e}$ in the vicinity of 1 . The amplitude has values very clearly higher than 1, on the order of 1.6 (Fig. 7), while, in the case described in the preceding section (which corresponds to Q→∞), the

amplitude becomes not so much more than 1, around 1.1. For some values of $\omega x/U_{0_e}$, the amplitude profile, moreover, has values clearly

11.

less than 1 toward the outside of the boundary layer. The theoretical elements developed by Patel, which are an extension of the methods of Lighthill, are valid for extreme values of the Strouhal number ($\omega x/U_{o_e} \to 0$ and $\omega x/U_{o_e} \to \infty$), do not allow explanation of these peculiarities. According to Patel, they must be associated with the fact that, when $\omega x/U_{o_e} = O(1)$, the inertial and frequency terms are of the same order of magnitude.

$$U_* = U_{*_0} + U_{*_1} \sin \omega(t - \tfrac{x}{Q})$$

$$U = U_0 + U_1 \sin[\omega(t - \tfrac{x}{Q}) + \Phi]$$
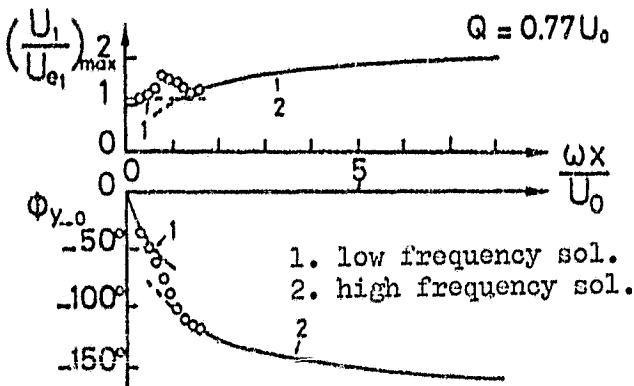
Fig. 7. Laminar boundary layer of flat plate perturbed by a progressive wave (from [33-36]).

The phase profiles indicate that the velocity in the boundary layer always is slower than the external velocity.

Two parameters compete to determine the phase distribution: velocity U_e and pressure gradient $-\frac{1}{\rho}\frac{\partial P}{\partial x}$. Now, the expression for this gradient is

$$-\frac{1}{\rho}\frac{\partial P}{\partial x} = \frac{\partial U_0}{\partial t} + U_e\frac{\partial U_e}{\partial x} = \omega U_{1e}\left(1 - \frac{U_{0e}}{Q}\right)\cos\omega(t \cdot \tfrac{x}{Q})$$
$$-\frac{\omega}{2}\frac{U_{1e}^2}{Q}\sin 2\omega(t \cdot \tfrac{x}{Q}) \qquad (22)$$

At low Strouhal numbers, the /6 velocity parameter prevails. The behavior of the boundary layer tends to become quasistationary, and the phase shifts are small. When ω increases, the pressure gradient parameter becomes large (Eq. 22). If U_{1_e}/U_{0_e} is small enough, the first term on the right side of (22) is dominant and, when convection velocity Q is smaller than U_0, the pressure gradient term lags 90° behind U_e. Besides, the interior of the boundary layer is more sensitive to the pressure gradient than the exterior, since the inertia is less. Therefore, this explains the negative phase shift values. This same reasoning explains why it is not paradoxical that the phase shift is positive when $Q \to \infty$ (see Section 3.3).

A singular situation results when $Q = U_0$, for the pressure gradient is zero in the first order. The solution proposed by Patel, for large values of $\omega x/U_{0_e}$, effectively indicates a change in behavior of the amplitude and phase profiles around $Q = U_0$ (Fig. 8).

12

3. Turbulent Flow

3.1. Experimental Results

$$U_e = U_{e_0} + U_{e_1} \sin \omega (t - \tfrac{x}{Q})$$

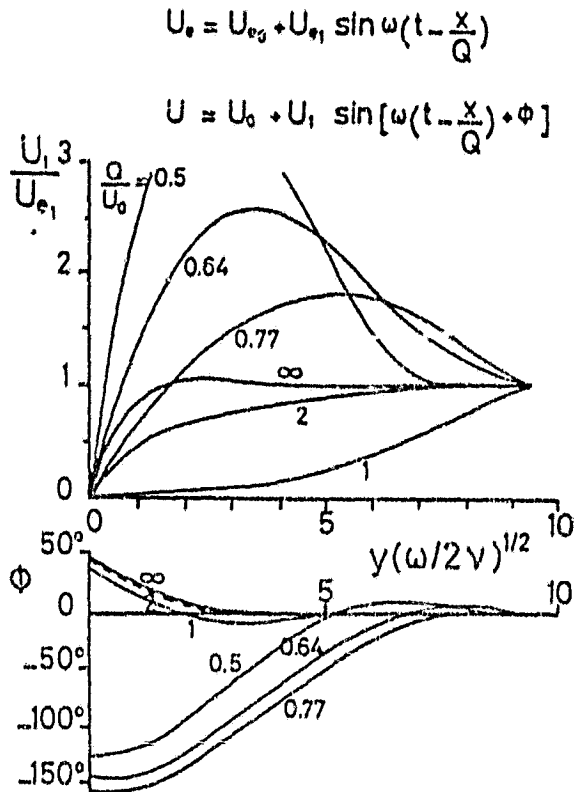$$U = U_0 + U_1 \sin [\omega(t - \tfrac{x}{Q}) + \phi]$$

Fig. 8. Effect of wave convection velocity (from [33-36]. High frequency theory $\omega x/U_{e_o} = 5$).

In turbulent flow, under-standing of unsteady effects is much less advanced than in laminar flow. The experimental efforts have concerned some particular points. Several studies have been devoted to oscillating flow around an average zero, with the effect of wall rough-ness. These studies often have been motivated by shear wave problems in the depths of the sea [21, 22]. The effect of pulsation on a boundary layer of a flat plate also has been studied [9, 23, 20, 11], but system-atic analysis of the various paramet which can affect the structure of the turbulence is still far from being achieved. In continuing study of laminar flow, M.H. Patel also has carried out an experiment in turbulent flow, on the effect of the phase velocity of the perturbation wave but, there also, the field of study remains largely open. Finally, very recently, several studies have been directed towards the effect of an average pressure gradient [3, 12-15, 24, 38, 41].

3.1.1. Oscillation Around an Average Zero

In Europe, studies of a turbulent boundary layer induced by oscil-lation imposed on the flow have evolved mainly in Denmark since the 1960s. Recently, Jonsson published an article which focuses on the group of studies carried out at the Technical University of Denmark. There, he also presents some outside results. The aim of the analysis is to demonstrate the existence of universal relations for the velocity

13

profiles, and to establish practical rules, especially for the coefficient of friction. The results are mainly for a rough wall.

Accordingly, Johsson was interested in flows, for which the exterior velocity is in the form

$$U_e = U_{1e} \cos \omega t \tag{23}$$

In the boundary layer, at the first harmonic, it is written

$$U = U_1 \cos(\omega t + \varphi) \tag{24}$$

We note that, since the flow is turbulent, it is advisable to define the average u correctly. This velocity is the average of a set and, when the flow is periodic, it also can be the phase average. Therefore, u is an average of the instantaneous values recorded in different cycles, for the same phase angle ωt within 2π.

Jonsson studied a deficit velocity, which he defined in complex form:

$$U_d = U_1 e^{i(\omega t + \varphi)} - U_{1e} e^{i\omega t} = U_{1d} e^{i(\omega t - \pi - \varphi_d)} \tag{25}$$

In a stationary turbulent boundary layer, conclusive progress has been made, due to the existence of a recovery region, where the velocity changes logarithmically. Under rough conditions, the rule of the wall is found by using the following reduced variables

$$U/U_\tau \quad \text{and} \quad y/k$$

where U_r is the friction velocity, $U_r = U_e(Cf/2)^{1/2}$, and k is the height of the roughness.

Jonsson attempted to verify such a logarithmic rule, by considering velocity U and friction velocity U_r at the same instant.

14

The friction velocity was determined from measurement of the velocity profile and by means of the summary equation of the momentum. This equation is quite simple. It results from the local equation which, in the case of parallel flow, is written

$$\frac{\partial U}{\partial t} = \frac{\partial U_e}{\partial t} + \frac{\partial}{\partial y} \frac{\tau}{\rho} \tag{26}$$

and it takes the form

$$\frac{\tau_p}{\rho} = \int_0^\infty \frac{\partial}{\partial t}(U_e - U)\, \partial u \tag{27}$$
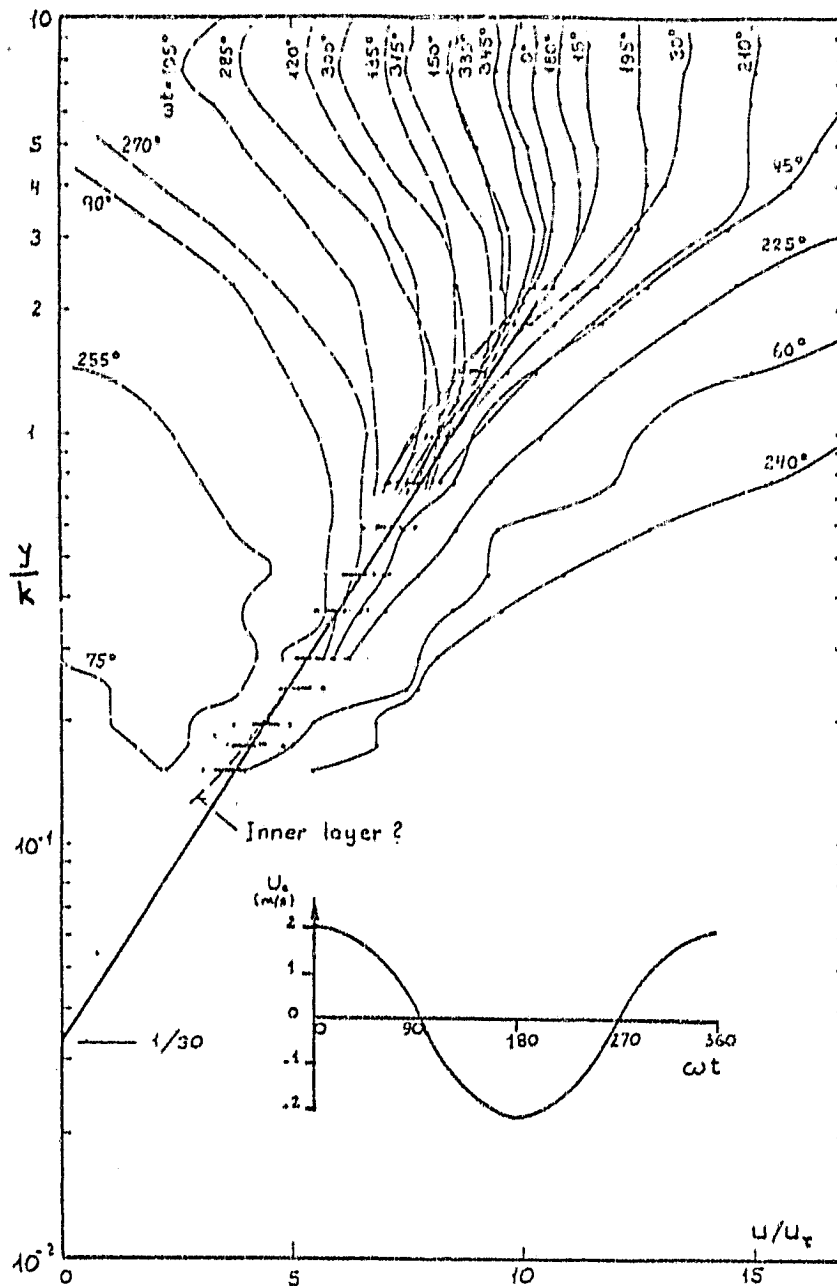
Fig. 9. Turbulent boundary layer oscillating around an average zero (from [21]).

15

Fig. 9 shows that, during a large part of the period, the measurements are grouped around the same curve as in stationary rough flow, of the equation $U/U_r = 5.75 \log(30y/k)$. Large deviations develop in the neighborhood of times when Ue is nullified.

Determination of the eddy viscosity ν_t shows that, in these same periods, ν_t has negative values, because of the inertia of turbulent friction $-\rho \langle u'v' \rangle$, with respect to the constraint $\frac{\partial U}{\partial y}$. Meanwhile, these periods remain quite limited and, for practical calculations, the utilization of a hypothesis of eddy viscosity should not be rejected a priori. In any case, it must be noted that the frequency imposed on the flow remains low with respect to the estimate which can be made of a characteristic frequency of the turbulence. This can explain why some classical results of stationary flow remain valid.

In a less convincing way, Jonsson also establishes the existence of a universal rule of deficit velocity, in the form

$$U_{1d}/U_{\tau max} = f_2(y/\delta)$$

(b is, by convention, the closest point of the wall, where the maximum velocity equals the maximum external velocity).

The existence of such a rule and of the rule of the wall, in the form $U/u_r = f_1(y/k)$, implies that of a rule of logarithmic recovery. Jonsson proposes /8

$$f_2 = 5.75 \log(1.13 y/\delta)$$

The extent of the recovery zone diminishes, when the ratio of the amplitude of the movement to the outside $a_{1e} = U_{1e}/\omega$ to the height of the roughness k decreases. This zone disappears, for values of a_{1e}/k on the order of 30.

It also must be noted that the existence of a rule of the wall $U/U_r = f_1(y/k)$ implies that the phase shift of the velocity in this region remains constant. In fact, it is enough to allow that U_r is in the form $U_r = U_{rm} \cos(\omega t + \phi_0)$, and the following is obtained

$$U = U_{\tau m} f_1(y/k) \cos(\omega t + \phi_0)$$

16

Experiment shows that, in the recovery region, the phase shift remains quite constant, but it appears to evolve in the viscous region under the layer. This then denies the existence of a rigorously universal rule in this underlying layer.

In order to permit complete construction of the velocity amplitude and phase profile, Jonsson found a representation of the phase profile of the deficit velocity ϕ_d. He proposes

$$\varphi_d = \frac{\pi}{2}\left(\frac{y}{b}\right)^{2/3}$$

Practical rules likewise have been proposed for the parietal coefficient of friction and the boundary layer thickness b. For thickness b, he proposes, under rough conditions,

$$b = 0.072\left(a_{1m}^3\, k\right)^{1/4}$$

Two conditions are distinguished for the coefficient of friction

$$\frac{a_{1m}}{k} < 1.6 \qquad \frac{\tau_{pmax}}{\rho\, U_{1e}^2} \approx 0.25 \text{ ou } 0.3$$

$$\frac{a_{1m}}{k} > 1.6 \qquad \frac{\tau_{pmax}}{\rho\, U_{1e}^2} = \frac{0.0605}{\log^2 22\frac{b}{k}}$$

Jonsson also has proposed formulas for the smooth condition

$$\frac{\tau_{pmax}}{\rho\, U_{1e}^2} = 0.09\, R_E^{-0.2} \qquad R_E = \frac{U_{1e}\, a_{1e}}{\nu}$$

$$\frac{b}{a_{1e}} = \frac{0.0465}{R_E^{0.1}} \qquad a_{1e} = \frac{U_{1e}}{\omega}$$

3.1.2. Oscillation Around an Average Nonzero Constant

In this section, we are interested mainly in the case of a boundary layer of a flat plate, perturbed by a sinusoidal oscillation of the external flow

$$U_e = U_{0e} + U_{1e}\cos \omega t \tag{28}$$

At the first harmonic, the velocity in the boundary layer is in the
form

$$U = U_0 + U_1 \cos(\omega t + \varphi) + \dots$$

(29)

As in Section 3.1.1., U is the average of the set of instantaneous
velocities. The difference between the instantaneous velocity and the
average of the set is the turbulent fluctuation u'. The moments, also
defined by the averages of the set, are designated $<u'^2>$, $<u'^3>$, and
the turbulent pressure is $-\rho<u'v'>$.

This problem is the basic circumstance of numerous practical situa-
tions, and many numerical solutions have been proposed over several
years. For a long time, the only supporting experiments were those of
Karlsson. Recently, others have published [9, 20, 11, 12]. The table
below gives the principal characteristics of the various cases studied.

	U m/s	δ H$_3$	$\frac{U_{1e}}{U_{0e}}$	x m	R_x millions	$S = \frac{\omega x}{U}$	$\sqrt{\frac{\langle u'^2\rangle}{U}}$ m/s
KARLSSON	4,57	0	0,30	2,5	0,75	0	6
	4,57	0,33	0,08 to 0,34	-	0,75	1,13	-
	5,33	0,66	-	-	0,88	1,94	-
	-	1,33	-	-	-	2,95	-
	-	2	-	-	-	3,92	-
	-	4	-	-	-	5,89	-
	-	7,65	-	-	-	11,80	-
	-	48	0,34	2,9	1,02	22,54 77,07	-
CHARNAY MELINAND	10	18,5	0,03 to 0,11	0,1 to 1,2	0,066 to 0,8	1,16 to 13,90	100 30
	10	18,5	0,20	0,1 to 1,2	0,066 to 0,8	1,16 to 13,90	50 20
	10	56	0,03 -0,2	0,9	0,6	31,70	25
HOUDEVILLE et al	85	40	0,34	0,55 sta.4	3,1	1,63	600
COUSTEIX et al(b,c)	33,60	41	0,37	0,55 sta.4	1,2	4,60	230

In this table, X designates the distance of the plate on which the
boundary layer is studied to the leading edge or, in the experiments of
Houdeville et al and Cousteix et al, the distance from the fictitious
origin of the boundary layer, calculated from the experimental data, on
the assumption that the average characteristics (in time) of the boundary
layer obey the stationary laws of the flat plate. A characteristic

frequency of the turbulence has been defined by $f_T = u'/\delta$, where u' is
a characteristic velocity of the turbulence, for example, $\sqrt{\overline{u'^2}}$.

In the experiments of Karlsson, the measurements provide average
velocity profiles U_o and profiles of in phase components $U_1 \cos\phi$ and out
of phase components $U_1 \sin\phi$. The experiments of Charnay and Melinand
give profiles of the average velocity, the average of the set U at
different instance of time in the period and some longitudinal and
transverse turbulence intensity profiles. In the experiments we have
performed, we measured the profiles of the average velocity U, which
are analyzed by means of harmonic decomposition, and we reported the U_o,
U_1 and ϕ profiles. Profiles of the longitudinal intensity of the
turbulence $<u'^2>^{1/2}$ and turbulent pressure $-\rho<u'v'>$ also were reported.
The density of probabilities of u' also was determined, as well as the
oblateness factor $F = <u'^4>/<u^2>^2$.

Average Velocity Profiles

The most evident conclusion of the experiments of Karlsson and
our experiments is that the average velocity profile U_o is practically
unaffected by the unsteady nature of the flow. However, it seems that
the experiments of Charnay and Melinand contradict these observations.
They particularly indicate an amplitude effect. Actually, for a
U_{1e}/U_{o_e} of 0.2 (f=18.5 Hz), the average velocity profiles clearly are
different ("squarer") than those obtained for $U_{1e}/U_{o_e} < 0.11$. For this
same value of the reduced amplitude, an 80% increase over the station-
ary case of the average thickness of the boundary layer has been measured,
as well as a 15% increase in the coefficient of parietal friction
(X=0.9 m, f=18.5 Hz). The observed effects on the average properties
of the boundary layer seem all the more surprising, that the experimental
conditions are approximately in the range of those studied by Karlsson.

In any event, if the effect of a turbulent perturbation of the
external flow [2, 8] and that of a harmonic perturbation are compared,
as Charnay and Melinand note, the effectiveness of the latter on the
average characteristics is very weak. The fundamental differences be-
tween the two types of perturbation must be emphasized. In one case, the

energy is distributed in a spectrum similar to that of turbulence, and it is a band in the other. We note that, in some cases studied by Karlsson, the frequency of the perturbation between the range of characteristic frequencies of the turbulence and the effect on the average profiles is not so large. The tridimensional and unidirectional natures of these two types of perturbation also must be compared.

Perturbation and Phase Amplitude

Qualitatively, the amplitude profiles we obtained and those of Karlsson have the same trend (Figs. 10, 11). In particular, they exceed the outer value in the external region of the boundary layer. These excesses can be on the order of 15 to 20%. When the Strouhal number increases, a layer similar to the Stokes laminar layer develops, of less and less thickness in the vicinity of the wall, and in which the amplitude variations are confined.
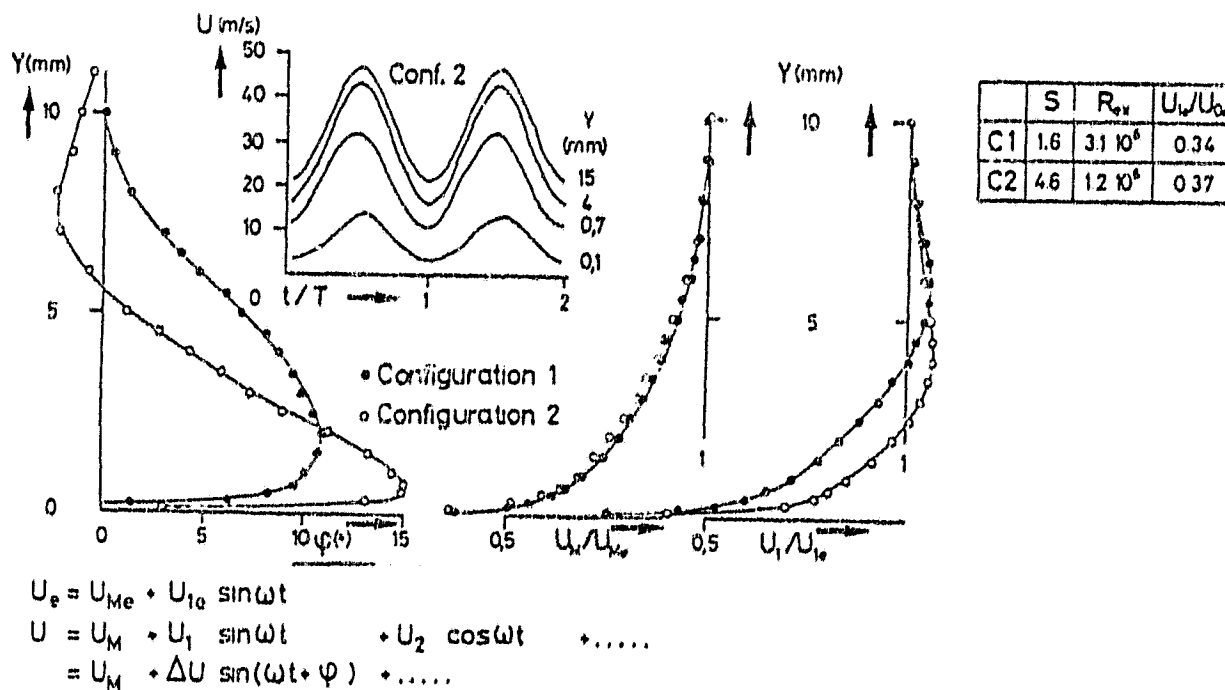

$$U_e = U_{Me} + U_{1e} \sin\omega t$$
$$U = U_M + U_1 \sin\omega t \quad + U_2 \cos\omega t \quad + \ldots$$
$$\quad = U_M + \Delta U \sin(\omega t + \varphi) + \ldots$$
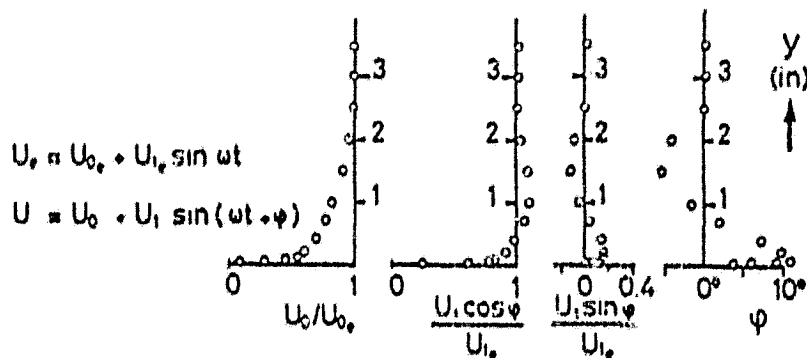
Fig. 10. Turbulent boundary layer in oscillating flow.

Fig. 11. Turbulent boundary layer in oscillating flow: $U_{1_e}/U_{o_e} = 34.4\%-\omega x/U_o = 3.92-R_{ex}=0.88\cdot10^6$ (from [23]).

The phase ϕ profiles are not given explicitly in the article of Karlsson, but they can be determined from the in phase component $U_1\cos\phi$ and the out of phase component $U_1\sin\phi$ profiles. With the scale on which these data are reproduced taken into account, some inaccuracy results from these analyses. Meanwhile, it appears that the results we obtained completely confirm these interpretations. Generally, it is observed that the phase is positive in a zone near the wall. As in laminar flow, this can be explained by the fact that the pressure gradient leads the external velocity by 90°, and that the less inert boundary layer in the vicinity of the wall responds more rapidly than the external flow. Toward the outside, significant negative values have been measured for some Strouhal numbers: 2.95, 3.92, 5.89 [23], 4.6 [11, 12]. For the other Strouhal numbers studied, the recorded values of ϕ toward the outside are generally within the experimental error. Similar observations have been made in laminar flow (measurements of Hill and Stenning, calculations of Farn, Arpaci and Clark). As a function of the Strouhal number, the lag of the phase maximum in the boundary layer is at a maximum for values of $\omega x/U_{o_e}$ on the order of 2.5-3.5. /10

It also is noted that variations of ϕ are established in a zone, which becomes thinner when the Strouhal number increases. At large Strouhal numbers, the outside of the boundary layer pulses as a unit. The phase shift is very small, and the amplitude is very close to the external value.

21

Phase Shift Relation Near the Wall

Finally, it is noted that the phase near the wall has a maximum and decreases at lower values of y. It is noted that the existence of a logarithmic recovery region implies that the phase shift must be constant and equal to its value at the wall [41]. It also can be shown here, by assuming that there is a universal rule near the wall, in the form

$$u^+ = f(y^+)$$
$$(u^+ = u/u_\tau, \quad y^+ = yu_\tau/\nu \quad u_\tau = u_e(c_f/2)^{1/2})$$

(30)

For this, we use the following complex notations

$$u_e = u_{0_e} + u_{1_e} e^{i\omega t}$$
$$\gamma = \gamma_0 + \gamma_1 e^{i\omega t} \qquad \gamma = (c_f/2)^{1/2}$$
$$u = u_0 + u_1 e^{i\omega t}$$

with u_{0_e}, u_{1_e}, γ_0, u_0 actual and γ_1 and u_1 complex. By assuming that u_{1_e}, γ_1 and u_1 are small compared to u_{0_e}, γ_0 and u_0, the rule $u^+ = f(y^+)$ can be developed, and the following are obtained

$$\frac{u_0}{\gamma_0 u_{0_e}} = f\left(\frac{y\, u_{0_e}\, \gamma_0}{\nu}\right)$$

(31)

$$u_1 = \gamma_0 u_{0_e}\left(\frac{u_{1_e}}{u_{0_e}} + \frac{\gamma_1}{\gamma_0}\right)\left(f\left(\frac{yu_0\gamma_0}{\nu}\right) + \frac{yu_0\gamma_0}{\nu}\frac{df}{dy^+}\right)$$

(32)

Formula (32) indicates that the phase ϕ of u is independent of y. It is such that

$$tg\, \varphi = \frac{\mathfrak{Im}\left(\frac{\gamma_1}{\gamma_0} + \frac{u_{1e}}{u_{0e}}\right)}{\mathfrak{Re}\left(\frac{\gamma_1}{\gamma_0} + \frac{u_{1e}}{u_{0e}}\right)}$$

Therefore, it is equal to the phase of $\gamma u_e = (\tau_p/\rho)^{1/2}$ and therefore, to that of the wall friction ε_p.

This conclusion is compatible with experiment, only in the region where the phase passes its maximum, and it can be thought that the interpretation of the variation of ϕ very close to the wall requires sharper analysis of the viscous underlying layer.

Meanwhile, it can be noted that the maximum of ϕ occurs in a region where the logarithmic rule is established in stationary flow (except for extreme very high values of the Strouhal number studied by Karlsson, $S=22.54$, $S=77.07$). We grant that the stationary rule remains valid at each instant

$$U^+ = \frac{1}{k} \ln y^+ + 5.25 \qquad k = 0.41$$

(33)

On the other hand, similarity solutions have been extended to the unsteady case, assuming a deficit velocity rule of the form $(U_e - U)/U_r = F'(y/\delta(x,t))$, and by accepting a quasistationary mixing length scheme [11]. It then is shown that friction can be calculated at each instant, by the relationship

$$\left(C_f/2\right)^{-1/2} = \frac{1}{k} \ln \frac{U_e \, \delta_1}{\nu} + D^*(G)$$

(34)

with

$$G = \frac{H-1}{H \, (C_f/2)^{1/2}} \qquad H = \frac{\delta_1}{\theta}$$

and

$$D^* = 2 G - 4.25 \, G^{1/2} + 2.12$$

A small perturbation hypothesis is then made, and it is written, in complex rotation

$$U = U_0 + U_1 \, e^{i\omega t}$$
$$U_e = U_{0e} + U_{1e} \, e^{i\omega t}$$
$$\gamma = \gamma_0 + \gamma_1 \, e^{i\omega t}$$
$$\delta_1 = \delta_{1_0} + \delta_{1_1} \, e^{i\omega t}$$
$$H = H_0 + H_1 \, e^{i\omega t}$$
$$\theta = \theta_0 + \theta_1 \, e^{i\omega t}$$

The expansion of relationships (33) and (34) then leads to

$$tg \, \varphi = \frac{(C+D) A_{\delta_1} \sin \beta_1 - D A_\theta \sin \varphi_\theta}{C + 1 + (C+D) A_{\delta_1} \cos \beta_1 - D A_\theta \cos \varphi_\theta}$$

(35)

with

$$A = \left(2 - \frac{4.25}{2 \, G_0^{1/2}}\right) \frac{H_0 - 1}{H_0} - 1 \qquad C = \frac{\gamma_0}{kA}$$

$$B = \left(2 - \frac{4.25}{2 \, G_0^{1/2}}\right) \frac{1}{H_0} \qquad D = \frac{B}{A}$$

23

ϕ_{δ_1} and ϕ_θ are phases of δ_1 and θ. A_{δ_1} and A_θ are the amplitudes of δ_1 and θ, reduced by the amplitude of U_e.

$$A_{\delta_1} = \frac{|\delta_{11}|/\delta_{10}}{U_{1e}/U_{0e}} \qquad A_\theta = \frac{|\theta_1|/\theta_0}{U_{1e}/U_{0e}}$$

The right hand term of Eq. (35) can be determined from experimental data. The value which the velocity phase should have in the logarithmic region then is determined. This phase should correspond to the maximum value determined experimentally, which alone is compatible with the theoretical result of $\phi=$este.

Comparison of the theoretical values thus determined with the experimental values is presented in Fig. 12. The results of Karlsson, unfortunately, could not be used, because the information is insufficient to calculate the right hand term of (35). Our results have been plotted in Fig. 12 [20, 11, 12]. Likewise, those obtained with an average pressure gradient [12-15] and those of M.H. Patel, who has studied the effect of the convection velocity of the perturbation wave, also have been plotted. The resulting agreement is altogether good, even for relatively high values of the Strouhal number, on the order of 6 to 7.

Fig. 12. Verification of proposed relationship for phase shift $\phi_u - \phi_{u_e}$ in the semilogarithmic region.
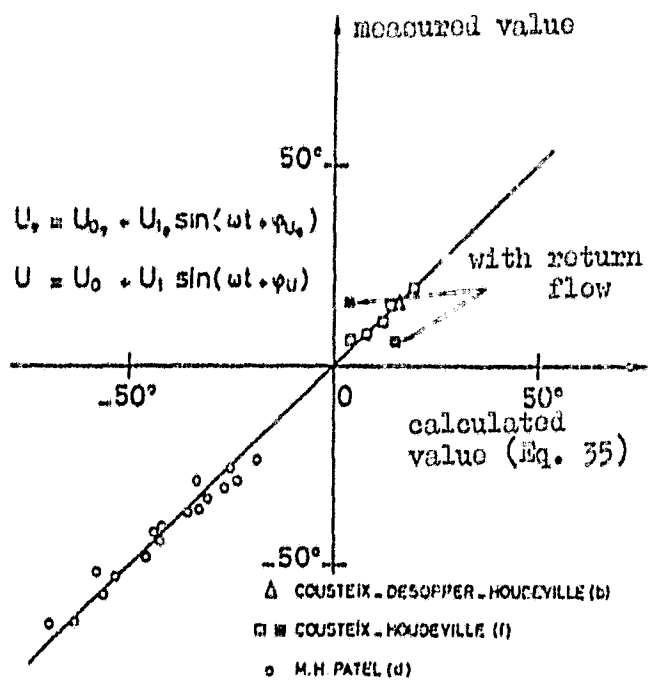
Effect on Turbulence Characteristics

In the experiments of Karlsson, only the average time value of the intensity of the turbulence was measured. It is impossible to detect a possible effect of frequency on these profiles, especially with the experimental error and the fact that higher order harmonics than 1 are included in the measurement taken into account.

The work of Charney and Mel'nand involved study of the free boundary and the velocities on the inside and outside of the turbulent bursts. It is evident that, for the stationary case, the indentations of the boundary are deeper and that, probably, the origin of the bursts is deeper inside the boundary layer. Unfortunately, this study is of too summary a nature, for analysis as a function of the phase has not been carried out and, under these conditions, it is difficult to make a distinction between the forced variations imposed on the free boundary by the pulsation of the flow and its random variation, which probably is a function of the phase.

More detailed measurements of the behavior of certain turbulent quantities have been reported by Cousteix et al, mainly in the second configuration, which corresponds to the highest Strouhal number. Measurements of the correlation coefficient $-<u'v'>/(<u'^2><v'^2>)^{1/2}$, which have an important role in modeling turbulence, have been carried out. They show that this coefficient evolves in the same way as in a stationary boundary layer (Fig. 13). Near the wall, within the measurement error, it can be considered that it is constant, with a value on the order of 0.45-0.5. Turbulent pressure measurements also have permitted determination of the experimental development of the mixing length $\ell=(-<u'v'>)^{1/2}/\frac{\partial U}{\partial y}$. This operation is a bit critical, for it requires calculation of the derivative $\partial U/\partial y$. However, it shows that, in the entire period, the mixing length evolves in the boundary layer in a very classical manner, except in a zone located in the vicinity of the external velocity maximum, where large variations are noted (Fig. 14).

It also is of interest to analyze the evolution of the oblateness /12 factor $F=<u'^4>/<u'^2>^2$, especially if it is interpreted as discontinuity factor γ, by using the relationship $\gamma=3/F$. We recall that γ, in unsteady flow, is a function of the distribution of the free boundary of the boundary layer. The $\gamma(y)$ curve (Fig. 15) depends on phase, and this dependence essentially expresses the forced variation of the boundary layer thickness. Actually, if y is plotted at $y_{\gamma=0.5}$ (the value of y for which $\gamma=0.5$), all the points are grouped, and they form a curve similar to that given by Klebanoff, in the case of the stationary boundary layer of a flat plate. This tends to show that the purely random
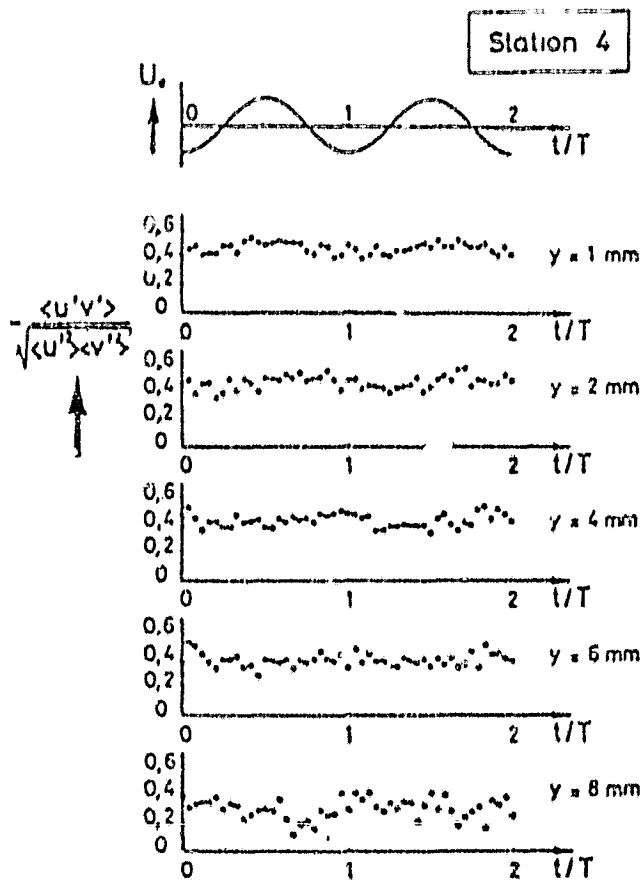
Fig. 13. Pulsed turbulent boundary layer, correlation coefficient.
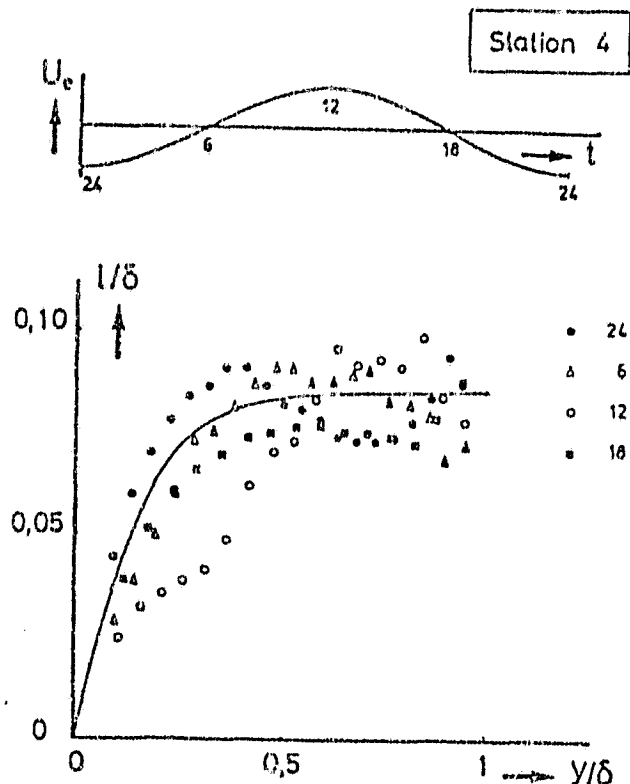

Fig. 14. Pulsed turbulent boundary layer, mixing length distribution.

variation of the free boundary is not affected by the unsteady nature of the flow.

Other measurements reported in detail by others [11, 12] tend to indicate a quasi-stationary behavior of the turbulence. However, it must be noted that the measurements were made under conditions, such that the frequency imposed is quite clearly less than the characteristic frequency of the turbulence f_T.

An estimate can be made of the conditions under which these two frequencies are of the same order of magnitude. A characteristic frequency of the turbulence is $f_T = u'/\delta$, where u' is a characteristic velocity of the turbulence, for example, $(\overline{u'^2})^{1/2}$. It can be estimated that the order of magnitude of u'^2 is given by $(r_p/\rho)/0.3$ (it is assumed that, near the wall, $-\overline{u'v'} = 0.3u'^2$). By using the flat plate formulas $C_f = 0.0368/R_x^{1/6}$ and $\delta/x = 0.25/R_x^{1/6}$, it is found that $f_T/f \simeq 2\pi R_x^{1/2}/S$. f_T and f are of the same order of magnitude, if $S = 2\pi R_x^{1/12}$. For Reynolds numbers of 10^6 to 10^7, this condition is satisfied for very high Strouhal numbers, on the order of 20. Under such
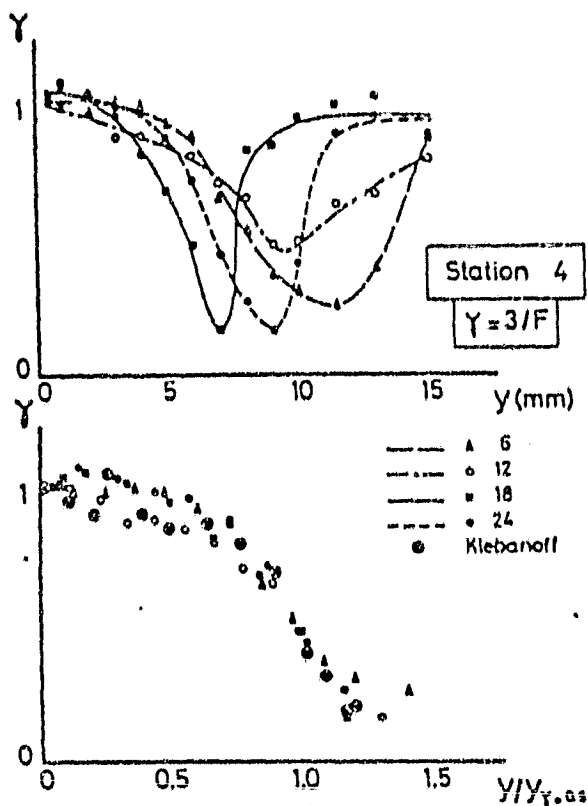
Fig. 15. Pulsed turbulent boundary layer, oblateness factor.

conditions, unsteady effects develop mainly in the underlying layer, and the bursting phenomenon can be affected. For higher frequencies, it can be asked whether a frequency does not exist, beyond which the unsteady effects on turbulence become very weak since, then, the unsteady layer is limited to an almost purely laminar zone near the wall.

3.1.3. Effect of Wave Convection Velocity

M.H. Patel [34-36] has developed, in turbulent flow, a study similar to that described for laminar flow in Section 2.4. The external velocity is in the form

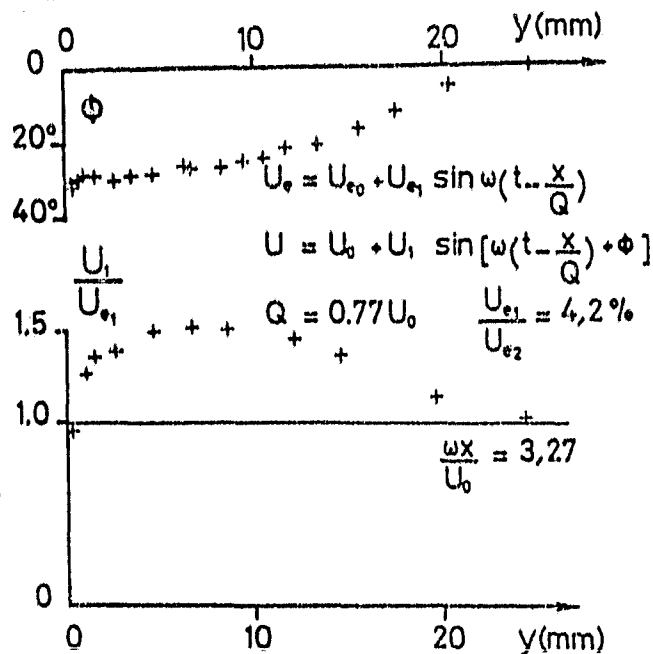$$U_e = U_{o_e} + U_{1e} \sin \omega(t - \frac{x}{Q})$$

with $\quad Q = 0{,}77 \, U_{o_e}$

The general conditions of the experiment are summarized in the table below.

$\frac{U_{o_e}}{m/s}$	$\frac{U_{1e}}{U_{o_e}}$	f	$\frac{x}{m}$	$\frac{\omega x}{U_{o_e}}$	R_x	$f_T = \overline{\sqrt{u^2}}/\delta$
19,8	3 % to 11 %	4 Hz to 12 Hz	1,288	1,64 to 4,91	$1{,}7.10^6$	
			1,516	1,92 to 5,77	$2 \quad 10^6$	55 Hz
			1,745	2,22 to 6,65	$2{,}3.10^6$	

It is noted that the imposed frequency is quite clearly different from the characteristic frequency of the turbulence.

The observed effects on the behavior of the average velocity, amplitude and phase profiles are qualitatively the same as in laminar

27

flow.   The average velocity profile is unchanged from the stationary case.   The amplitude exceeds its exterior value (Fig. 17), and the reduced amplitude maximum U_{1e}/U_{oe} increases with the Strouhal number (Fig. 16) (it is 1.77 for S=6.65).

Fig. 16.   Boundary layer of flat layer perturbed by progressive wave (from M.H. Patel).

It is noted that the Strouhal numbers studied are larger than those in the study conducted of laminar flow, and that the singular results obtained around S=1 were not observed in turbulent flow.

As in laminar flow, the phase shift in the boundary layer always is negative (Fig. 17). The absolute values of the phases sometimes are smaller in turbulent flow (Fig. 16).   As was discussed in Section 2.4, two parameters come into play for the phase shift behavior: velocity and pressure gradient.   Given that the turbulent boundary layer is less sensitive to the pressure gradient than a laminated boundary layer, it is logical that the phase shifts are smaller than in a turbulent boundary layer.

Finally, we note that, in a large part of the boundary layer, ϕ remains nearly constant (Fig. 16).   This result is completely compatible with the existence of a universal rule $u^{+}=f(y^{+})$ (see Section 3.1.2).   We recall that the values of these phases were compared to the theoretical values, calculated by Eq. (35) (Fig. 12).

Likewise, M.H. Patel measured the longitudinal intensity of the average turbulence over time.   No effect of the pulsation was recorded.   /13 Within experimental error, the profiles are identical to those of stationary flow.

28

$$U_{\bullet} = U_{\bullet 0} + U_{\bullet 1} \sin \omega\left(t - \tfrac{x}{Q}\right)$$

$$U = U_0 + U_1 \sin\left[\omega\left(t - \tfrac{x}{Q}\right) + \phi\right]$$
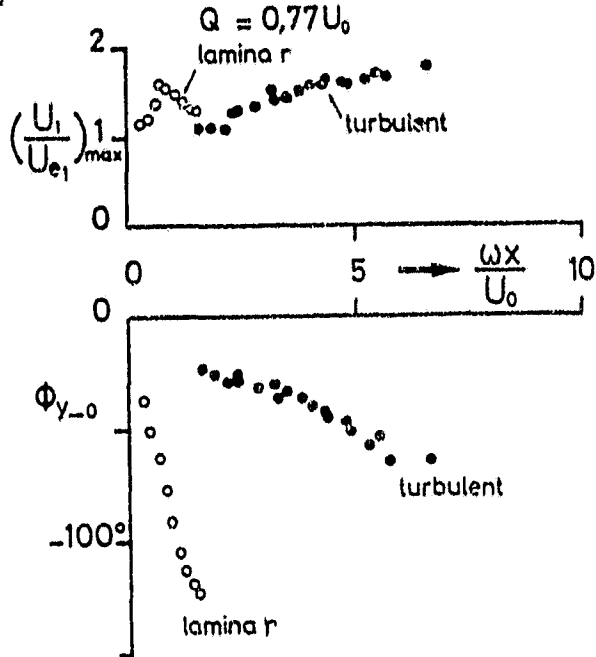
$$Q = 0{,}77 U_0$$

Fig. 17. Turbulent boundary layer of flat plate perturbed by progressive wave (from M.H. Patel).

3.1.4. Effect of Average Unfavorable pressure gradient

Several experiments now are under way or planned, to study the effect of pulsations on a boundary layer exposed to an average pressure gradient [38, 41, 22, 3, 12-15]. The principal characteristics of these experiments are summarized in the table below

	U m/s	ϕ H$_y$	$\frac{U_{Ac}}{U_{0c}}$	x m	R_x	S	$\frac{u'_1}{H}$
SCHACHENMANN ROCKWELL	29	7.5	0,069	0.2	$0.37 \cdot 10^6$	0,33	330
	17	33	0,013	0,42	$0.22 \cdot 10^6$	2,44	200
Conical diffuser, total divergence 6°, length 0.615 m.							
SIMPSON	15	0,596	0,30	0	0	0	
	22	-	0,30	1.5	$2.18 \cdot 10^6$	0,255	50
	15,8	-	0,30	3.0	$3.13 \cdot 10^6$	0,711	
Boundary layer studied on flat platform of convergent-divergent jet.							
VENISON	22	0 to 6	0,02 to 0,08	0,75 to 1,75	$1.09 \cdot 10^6$ $1.8 \cdot 10^6$	0 to 1,210 0 to 4,230	75
	15,6						
Study on flat plate with trailing edge flat. Wave convection velocity $Q=0.65 U_0$.							
COUSTEIX HOUDEVILLE	30	38	0,20	0.35	$0.7 \cdot 10^6$	28	230
	20,4	-	0,10	0.95	$1.3 \cdot 10^6$	11	60
Study on jet platform. Pressure gradient induced by a section.							
BINDER et al.	0,11 to 0,48	0 to 1,36 / 0 to 1,36	0,04 to 0.50 / 0,04 to 0.50	1 to 2 / 1 to 2	$7.3 \cdot 10^4$ to $1.45 \cdot 10^5$ / $3.2 \cdot 10^5$ to $6.3 \cdot 10^5$	78 / 18	0,3 / 1,53
Flat diffuser, total aperture up to 30°. Length 1m, hydraulic cell.							

In the above table, X=0 corresponds either to the leading edge of the plate on which the boundary layer was studied [24, 41], or to the fictitious origin of the turbulent boundary layer, determined from the experimental results at the first measurement station [38, 12-15], or estimated [3].

It is noted that the use of a hydraulic cell [3] is a good means of easily obtaining high Strouhal numbers and pulsation frequencies, which are in the range of the characteristic frequencies of the turbulence.

In the experiments reported by Kenison, no unsteady effect was noted on the evolution of the average characteristics of the boundary layer over time: velocity profiles; coefficient of friction; density of momentum; shape parameter, intensity of turbulence even in vicinity of point $C_f=0$ (Fig. 18). Upstream from $C_f=0$, a zone develops, where the velocity periodically is negative. This zone remains thin, and the rough thickening of the boundary layer is observed practically in the same zone as in stationary movement.

The amplitude and phase profiles also were measured by Kenison. The phase profiles indicate tendencies associated with phase shifting of the pressure gradient $\frac{\partial P}{\partial x}$ with respect to the external velocity. The phase shifts in the boundary layer are more pronounced than in the case U_o=cste. This can be explained by the fact that, in the vicinity of the /14 breakaway, the velocity near the wall is much lower, and the inertia, therefore, is much weaker.

The experiments of Schachenmann and Rockwell in a conical diffuser with a 6° total aperture indicate that the average characteristics of the boundary layer are not affected by variation of the pulse frequency. The average pressure recovery coefficient is not affected either. Preliminary tests conducted by Binder et al with much higher Strouhal numbers lead to identical conclusions, as long as the boundary layer is not separated ($2\alpha<7^o$). For larger apertures, very noticeable improvements in yield are obtained by increasing the frequency. It must be noted that, in these tests, the external velocity frequency and amplitude varied at the same time, and it is impossible to separate the
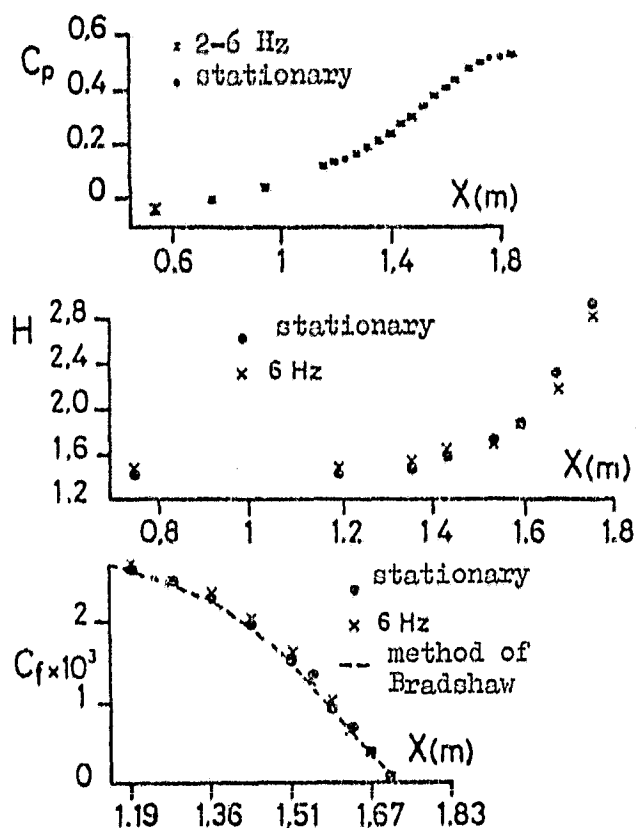
30

Fig. 18. Turbulent boundary layer exposed to average pressure gradient perturbed by progressive wave (from Kenison).

effects due to frequency and those due to amplitude. Very strong relative amplitudes were obtained up to 1.24. In addition, this problem brings into play coupling between the external flow and the boundary layer.

The tests reported by Simpson were carried out at low Strouhal numbers and at low frequencies, compared with the characteristic frequencies of the turbulence. The first results published in this study mainly concern the average set velocity, amplitude and phase profiles. At the station presented, it was found, in particular that the average set velocity profiles all have a semilogarithmic region, in which the phase is practically constant. The great thickness of the boundary layer has permitted precise determination of the phase variations in the underlying layer. These soundings confirm the very high sensitivity to unsteady effects, and they show that phase ϕ varies very rapidly.

The first results we obtained on the effect of unsteadiness on a boundary layer subject to a pressure gradient were presented in detail during this colloquium. In particular, data obtained by means of a laser anemometer in a zone with back flow are described there. As this zone develops, the unsteady effects become larger. For example, during one period, the shape factor at the last measurement station varies between 2 and 5. When the shape factor is raised, very noticeable modifications of oblateness factor F are noted. In particular, F increases

in the vicinity of the wall. Meanwhile, it was verified that the
average set velocity profiles at each instant of the period can be rep-
resented by profiles, drawn from a family established in the stationary
state, in the outer region of the boundary layer (Fig. 19). This was
observed, as long the instantaneous profile did not have a negative
velocity (H<2-2.3), up to Strouhal numbers on the order of 6 to 7.
Likewise, the existence of a semilogarithmic region could be observed
at each instant during the period, the extent of which decreased, as in
stationary flow, when the shape factor increased. It practically dis-
appeared when H was on the order of 2 to 2.3. In this region, the
velocity phase angle in the boundary layer, with respect to the external
velocity, has an extreme, the value of which has been compared to the
theoretical value given by Eq. (35) (Fig. 12). Good agreement is obtained,
up to the time when the average velocity of the set becomes negative in
a small portion of the period. Here again, rapid variations of the
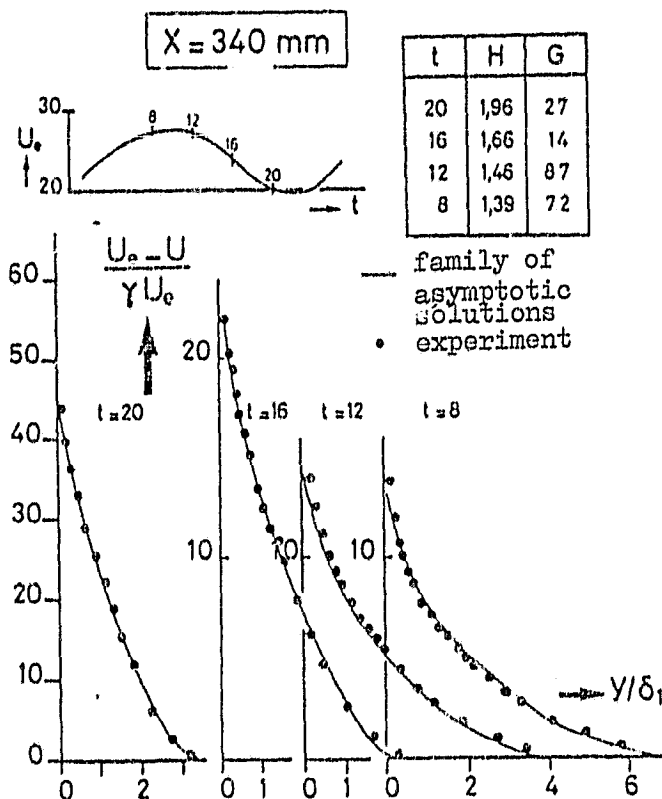phase angle were recorded near the wall.

Fig. 19. Pulse turbulent boundary
layer with average pressure gradient;
comparison of instantaneous velocity
profiles to theoretical family.

3.2. Calculation of Boundary Layer

Most of the methods pro-
posed and actually used are
extensions, frequently very
direct, of those perfected in
stationary flow. Two types of /15
methods are distinguished, with-
out comparison: methods of solu-
tion of local equations and
methods of solution of global
equations.

3.2.1. Proposed Methods

In the first type of method,
the basic equations to be solved
are local equations of continuity
and momentum, which are derived

32

from Navier-Stokes equations (1) and (2). The instantaneous velocity
is broken down into the average of the set u_i and the turbulent fluc-
tuation u'_i. After applying this breakdown in equations (1) and (2),
forming the average of the set of equations obtained and using the
boundary layer hypotheses, the following is obtained

$$\frac{\partial u}{\partial x} + \frac{\partial v}{\partial y} = 0 \tag{36}$$

$$\frac{\partial u}{\partial t} + u\frac{\partial u}{\partial x} + v\frac{\partial u}{\partial y} = -\frac{1}{\rho}\frac{\partial p}{\partial x} + \frac{\partial}{\partial y}\left(\mu\frac{\partial u}{\partial y} - \rho\langle u'v'\rangle\right) \tag{37}$$

Different turbulence schemes have been tested. The simplest are
the "zero equation models," eddy viscosity [45-48, 7] or the mixing
length models [10-15]. These models are identical to those used in
stationary flow. For example, the mixing length model is written

$$-\langle u'v'\rangle = \ell^2\left(\frac{\partial u}{\partial y}\right)^2 \tag{38}$$

where $\ell/\delta(x,t)$ is the same function as in stationary flow

$$\frac{\ell}{\delta} = 0.085 \, th\left(\frac{0.41}{0.085}\frac{y}{\delta}\right)$$

Near the wall, corrections are introduced to allow for viscosity
effects.

Several other authors have used a one equation model for the
Reynolds stress [4, 42, 32]. A two equation model for the kinetic
energy and dissipation also have been used [10-15]. In these models,
only the convection term is modified, by including the time derivative.
For example, the two equation model is written

$$\frac{Dk}{Dt} = -\langle u'v'\rangle\frac{\partial u}{\partial y} - \varepsilon + \frac{\partial}{\partial y}\left(\frac{C_\mu}{\sigma_k}\frac{k^2}{\varepsilon}\frac{\partial k}{\partial y}\right) \tag{39}$$

$$\frac{D\varepsilon}{Dt} = -C_{\varepsilon_1}\frac{\varepsilon}{k}\langle u'v'\rangle\frac{\partial u}{\partial y} - C_{\varepsilon_2}\frac{\varepsilon^2}{k} + \frac{\partial}{\partial y}\left(\frac{C_\mu}{\sigma_\varepsilon}\frac{k^2}{\varepsilon}\frac{\partial\varepsilon}{\partial y}\right) \tag{40}$$

$$-\langle u'v'\rangle = C_\mu\frac{k^2}{\varepsilon}\frac{\partial u}{\partial y}$$

In the second type of method, the local equations are integrated
over y. In general, they use the integral equation of momentum

$$\frac{C_f}{2} = \frac{\partial \theta}{\partial x} + \theta \frac{H+2}{U_e} \frac{\partial U_e}{\partial x} + \frac{1}{U_e^2} \frac{\partial}{\partial t}(U_e \delta_1) \tag{41}$$

and, frequently, an auxiliary equation, which can be the integral
equation of continuity

$$\frac{\partial \delta}{\partial x} - \frac{v_e}{U_e} = \frac{1}{U_e} \frac{\partial}{\partial x} U_e (\delta - \delta_1) \tag{42}$$

or the integral equation of average kinetic energy

$$\frac{\partial \delta_3}{\partial x} + 3 \frac{\delta_3}{U_e} \frac{\partial U_e}{\partial x} + \frac{1}{U_e} \frac{\partial}{\partial t}(\delta_1 + \theta) + \frac{1}{U_e^3} \frac{\partial}{\partial t} U_e^3 = \frac{2}{\rho U_e^3} \int_0^\delta \tau \frac{\partial u}{\partial y} dy \tag{43}$$

or, again, an equation of momentum, obtained by multiplying the local
equation of momentum by y

$$\int_0^\delta y \frac{\partial u}{\partial t} dy + \int_0^\delta \left[2yu - \int_0^y u\, dy + \int_0^y (v - v_e)\, dy \right] \frac{\partial u}{\partial x} dy$$

$$= \frac{1}{2}\left(\frac{\partial v_e}{\partial t} + U_e \frac{\partial U_e}{\partial x} \right) \delta^2 - \frac{1}{\rho} \int_0^\delta \tau\, dy \tag{44}$$

Whatever the auxiliary equation used, it is necessary to have
available supplementary relationships to solve the integral equations,
since they bring out an excessive number of unknowns. These closure
hypotheses are relationships between the integral quantities brought
out by integration of the local equations.

McDonald and Shamroth solve equations (41) and (43). The supple-
mentary relationships are obtained, by assuming that the average set
velocity profile can be represented at each instant by a Coles profile.
The coefficient of dissipation was calculated, by expressing friction
by means of a mixing length scheme.

In the method proposed by Kuhn and Nielsen, the basic systems are
equations (41) and (44), which are solved after linearization, by
assuming that the unsteady perturbation is weak. The supplementary re-
lations were obtained by assuming that, at each instant, the velocity
profile is described by a Coles profile.

M.H. Patel has analyzed two methods. Each solves linearized equa-
tions, obtained by assuming a small unsteady, harmonic perturbation. In

34

the first method, the average flow is calculated by a stationary method,
for example, the method of Green. With the average flow known, the
oscillatory perturbation can be calculated, based on two hypotheses:
1. at each instant, the wall friction can be calculated by a stationary
rule (the Ludwieg-Tillmann law, for example); 2. the in phase and out of
phase components of the velocity are represented by

$$\frac{U_1 \cos\varphi}{U_{1e}} = \eta^{1/9} + R(\eta^{1/3} - \eta) \tag{45}$$

$$\frac{U_1 \sin\varphi}{U_{1e}} = S(\eta^{1/3} - \eta) \tag{46}$$

Patel has obtained these profiles from his experiments. These
expressions were utilized to calculate the perturbations of the
integral densities. R and S thus become the main unknowns in the integral
equations, and the solution provides their values.

In the second method analyzed by Patel, it simply is assumed that,
at each instant, the supplementary relations used in the method of
Green remain valid.

The method proposed by Cousteix et al [11-13] likewise is an
extension of the method first established in stationary flow [31]. The
basic system is made up of the integral equations of momentum (41) and
continuity (42). The closure relationships are obtained, after deter-
mination and analysis of the similarity solutions (similar in spirit to
the stationary solutions of Falkner and Skan of laminar flow). It is
assumed that the deficit velocities obey a similarity rule of the form
$(U_e - U)/U_r = F'(y/\delta(x,t))$, and the friction is calculated by a mixing
length model. It then is shown that the resulting family of profiles
is strictly identical to that determined in stationary flow. It
depends uniquely on the Clauser parameter:

The set of closure relationships necessary to solution of the integral
equations is then deduced:

one rule for the δ_1/δ ratio

$$\frac{\delta_1}{\delta} = \gamma \, F_1(G) \qquad \gamma = (C_f/2)^{1/2} \tag{47}$$

one rule for the wall friction

$$\frac{1}{\gamma} = \frac{1}{k} \ln R_{\delta_1}^2 + D^*(G) \quad k = 0.41 \tag{48}$$

one rule for the drive coefficient

$$\frac{\partial \delta}{\partial x} - \frac{V_e}{U_e} = \gamma P(G) - \frac{1}{U_e} \frac{\partial \delta}{\partial t} \tag{49}$$

With respect to the stationary case, only the relationship for the drive coefficient is modified.

F_1, D^* and P are functions of G, determined by the similarity solutions

$$F_1 = 0.613\, G - (3.6 + 76.86(1/G - 0.154)^2)/G$$
$$D^* = 2\, G - 4.25\, G^{1/2} + 2...$$
$$P = 0.074\, G - 1.0357/G$$

3.2.2. Application of Different Methods

Despite the large number of publications on calculation of unsteady turbulent boundary layers, it is difficult to compare the performance of the various proposed methods. Frequently, the methods have been applied to purely theoretical cases, and the various authors have not taken up the same cases. L.W. Carr recently proposed standardization of these examples. Without being devoid of interest, such exercises, meanwhile, are of only relative value. One method is compared with another, and it is quite clear that no universally valid method exists in turbulent flow. Only systematic comparison to experiment permits determination of the field of validity of a method. Therefore, here, we limit outselves to reporting some results of such comparisons.

At present, the most complete example is that of a boundary layer of a flat plate exposed to a harmonic perturbation. A comparison with available experimental data is presented in Fig. 20. We note that the Strouhal number is not the unique parameter of the solution. The Reynolds number and the amplitude of the fluctuations can play a part.
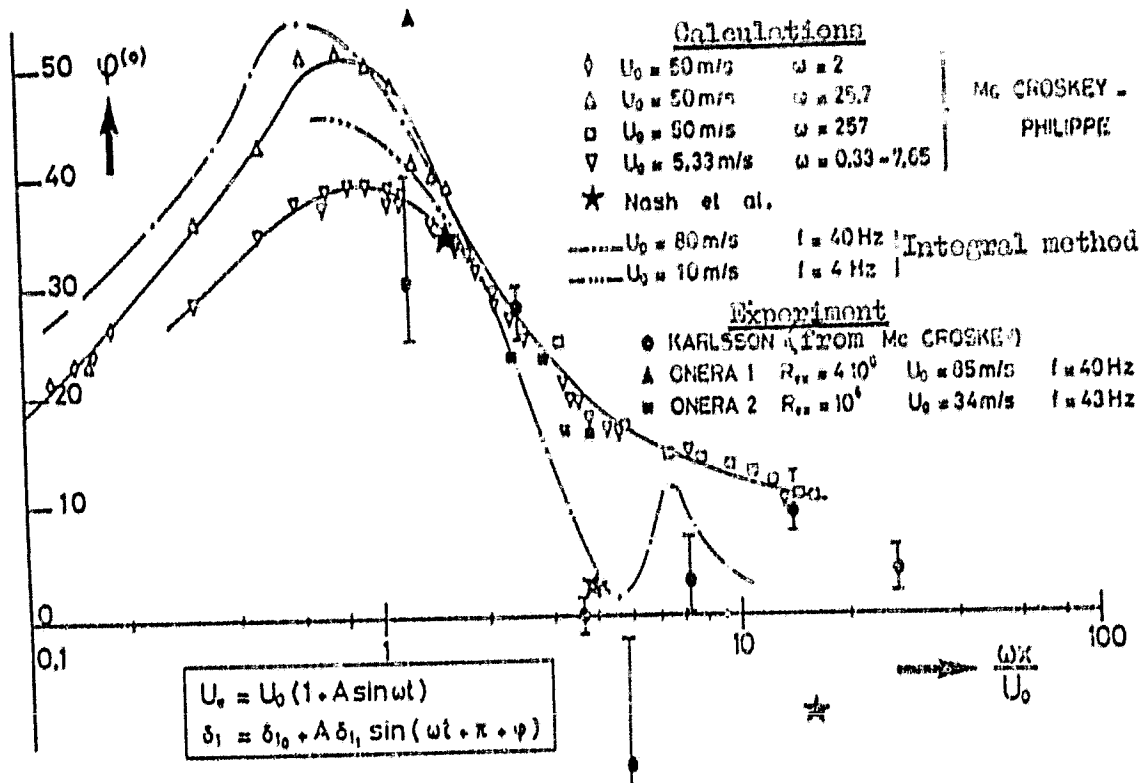
36

Fig. 20a.   Calculation-experiment comparison: average zero
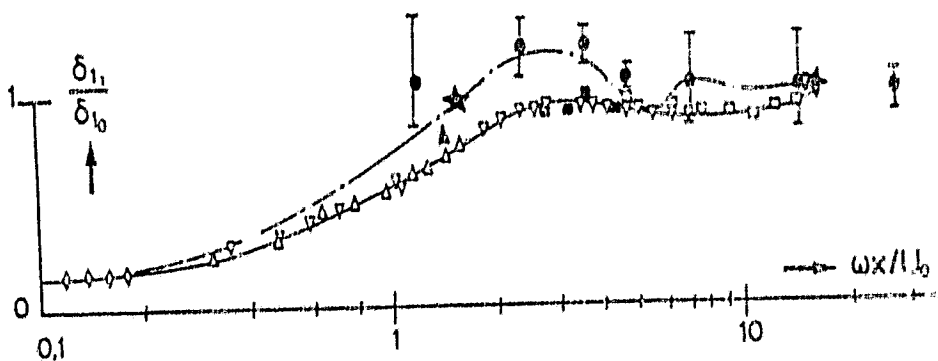pressure gradient; phase of δ_1.

Fig. 20b.   Calculation-experiment comparison: zero
average pressure gradient; amplitude of δ_1.

It appears that, for intermediate Strouhal numbers in the 1 to 5 range, the various calculations are not too different from experiment. For large Strouhal numbers, there is a major difficulty. It is the modeling of turbulence in the viscous underlying layer. Actually, when the Strouhal number is very large, the unsteady effects are included in a very thin layer near the wall, and prediction of them is essentially associated with modeling of the underlying layer, and this problem is part of that of the interaction between the forced pulsation and turbulence, since the forced frequency is in the range of the characteristic frequencies of the turbulence. Acharya has carried out experiments with pulse flow in a duct, in which the amplitude and phase variations of the velocity are located mainly in the underlying layer. The calculation tests he presents effectively indicate difficulties.
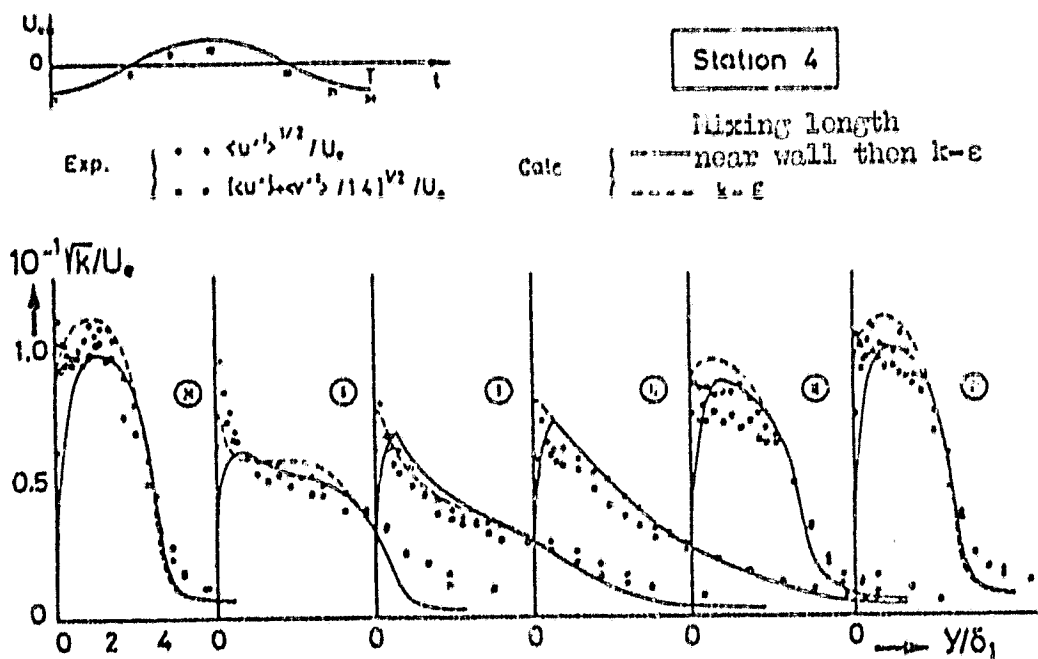

Fig. 21. Calculation-experiment comparison: intensity of turbulence.

We present a comparison of turbulence intensity and turbulent pressure profiles we have obtained in Figs. 21 and 22. With the experimental dispersion, especially of $\langle u'v' \rangle$, taken into account, it is difficult to state which of the methods used is better. However, it appears that the mixing length model predicts the deformation of the $\langle u'v' \rangle$ profiles more poorly, especially at instants 9 and 12, located at the external velocity maximum.
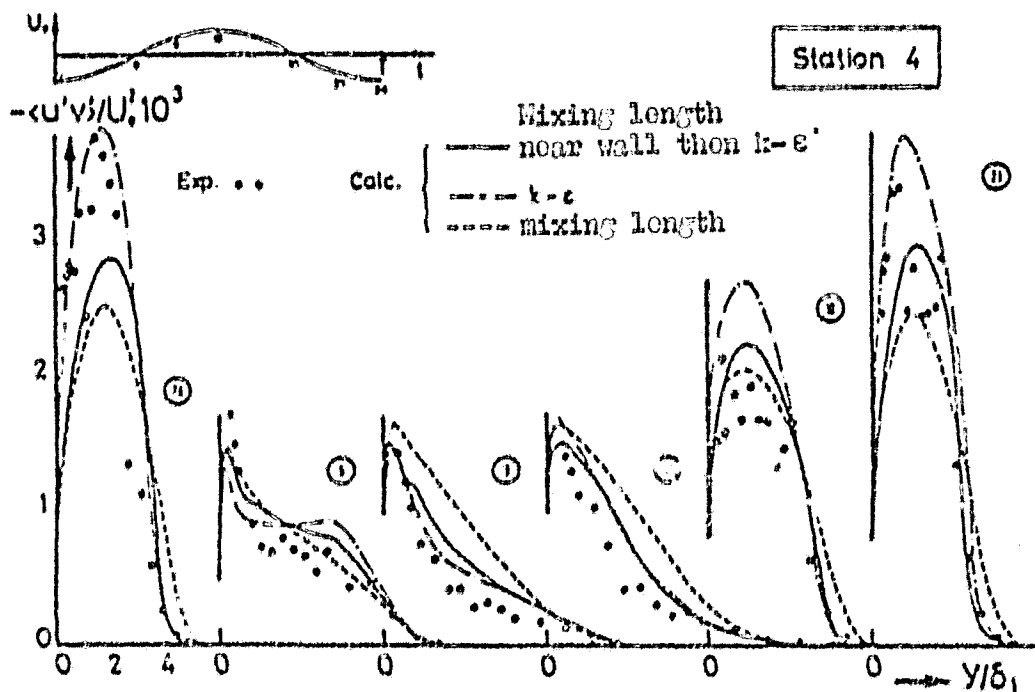
38

Fig. 22. Calculation-experiment comparison: turbulent pressure.

Figs. 23 and 24 show a comparison of the experiments of M.H. Patel. The different calculations were carried out with integral methods. Up /18 to the highest Strouhal number (6.65), good agreement with experiment is obtained, the phase deviations certainly are not significant, with the difficulty of determining them experimentally with precision taken into account. In any case, a small dispersion must be noted in the theoretical results for the largest Strouhal numbers.

Finally, Fig. 25 presents a comparison of the first results we obtained with the average pressure gradient. The calculations, carried out by the integral method, are interrupted at the station where a /19 return flow appears. Actually, extension of the calculation area in the recirculation region requires that certain conditions at the limits along the boundary downstream of the area be taken into account.

3.2.3. Breakaway problem. Formation of Singularities in the Boundary Layer Calculation.

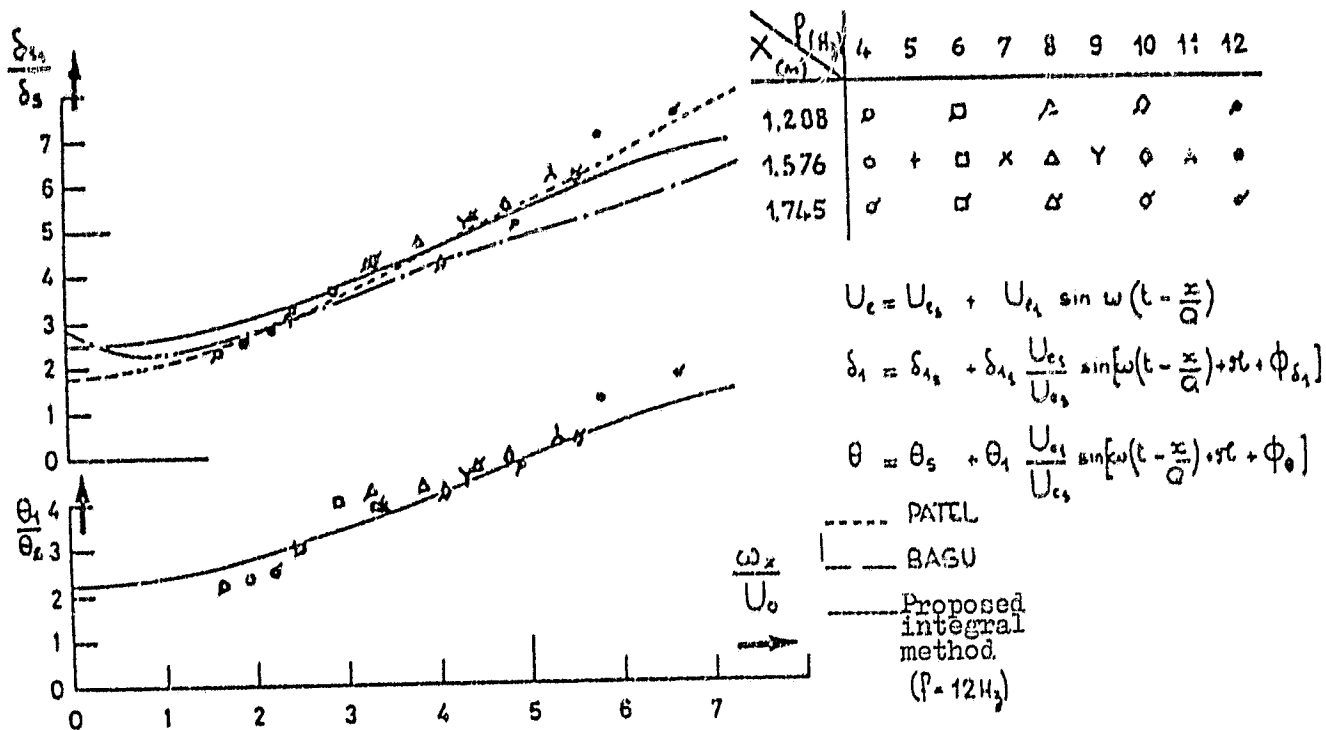The breakaway problem raises numerous other questions, and it still

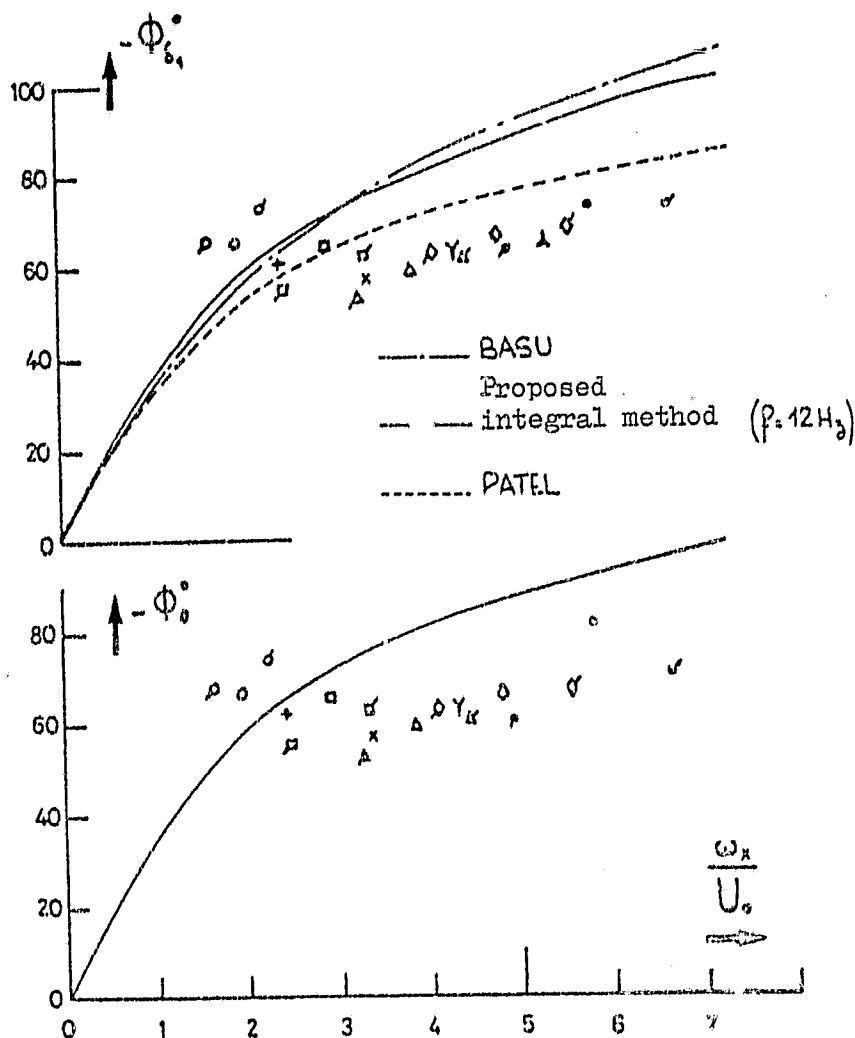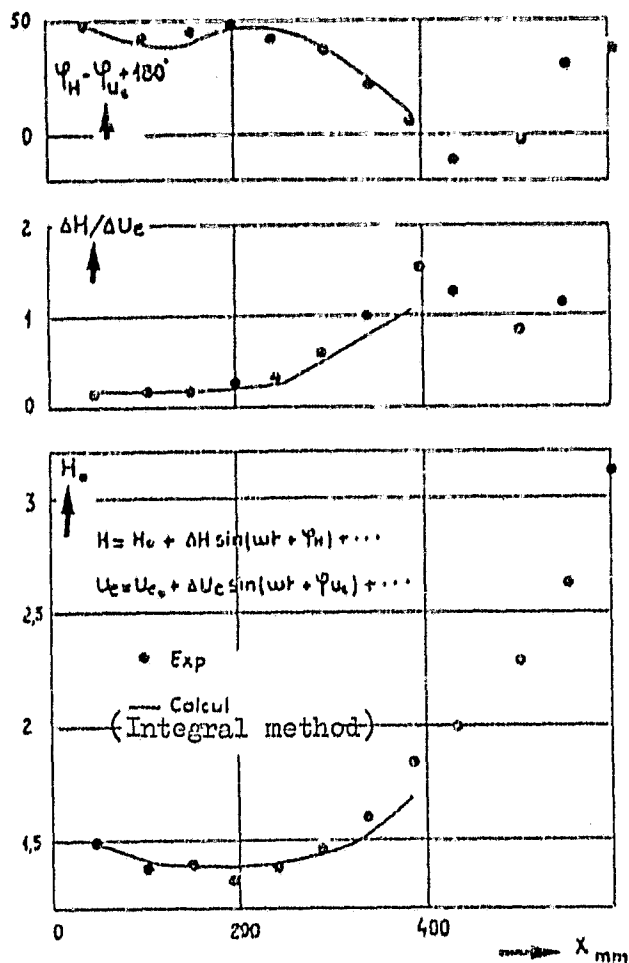Fig. 23. Comparison of experiments of M.H. Patel.

Fig. 24. Comparison of experiments of M.H. Patel.

40

Fig. 25. Calculation-experiment comparison: pulsed turbulent boundary layer with average pressure gradient.

is not resolved, even in laminar flow.

The only certain proposition is negative. Breakaway is not necessarily connected to point $Cf_1 = 0$, as in stationary flow. It must be emphasized that confusion frequently has occurred over the word, breakaway, since some authors. have, by definition, connected this word to the fact that $Cf = 0$. Rather, it must be reserved to signify catastrophe (breakaway, breakdown) for the boundary layer equations, by which the very notion of boundary layer ceases to be valid.

Several authors have proposed breakaway criteria, principally in laminar flow. We first mention that of Moore, Rott and Sears [39], established for the case of stationary flow with a mobile wall

($U_p \neq 0$). Breakaway develops at a point where the velocity is zero and where the gradient also is zero. This problem is a special case of unsteady flow because, in a reference system connected to the wall, the flow is quite unsteady, and it has been proposed [39] to use a similar criterion in the general case. However, numerical studies have shown that a singularity does not always occur at this point.

A more global approach to this problem, always in laminar flow, has been studied by Shen and Nenni, who found the existence of a singularity, by a noncoincidence condition between the boundary layer and the potential flow. This condition is expressed by the fact that the vertical velocity becomes not limited at the boundary of the boundary layer.

41

They have shown that the wall friction behavior gives an indication of this condition. Besides, they have shown that the wall friction obeys a Burgers type equation

$$\tau_y = \frac{h_1 \rho}{\rho_2 \rho} \tau_y + \frac{x \rho}{h_2 \rho} \eta_2 + \eta_2 \tau_y \tag{50}$$

h_1, h_2 and h_3 are functions of x and t.

Therefore, it clearly appears that point $r_p = 0$ does not, a priori, play any special part, except in stationary flow ($\frac{\partial}{\partial t} = 0$), where a Goldstein type singularity then is found for r_p, which varies as the square root of x. In unsteady flow, the formation of singularities must be found elsewhere, in the form of a discontinuity by development of a shock wave.

Comparable results have been found by Cousteix et al in the turbulent case, by analyzing the properties of the integral equations (equation of continuity and of momentum), to which closure relationships (47), (48) and (49) are added. It leads to the following conclusions:

the system always has two real characteristic directions λ_1 and λ_2 ($\lambda = dx/u_e dt$); it is hyperbolic;

one of the directions, λ_1, is always such that $0 < \lambda_1 < 1$;

the 2nd direction, λ_2, is positive for values of the form factor less than a critical value H_c ($H_c \approx 2.6$); it is negative for $H > H_c$.

It also is shown that point $H = H_c$, in practice, is confused with point $C_f = 0$. Therefore, the result is that the formation of singularities is not connected with point $C_f = 0$. When λ_2 becomes negative, this signifies that information is transmitted from downstream to upstream.

The development of singularities occurs by the formation of shock fronts, across which the characteristics of the boundary layer are discontinuous. It is clear that the hypotheses themselves of the

boundary layer, then, are defective. It can be thought that, as in stationary flow, coupling with the external flow must be resorted to, in order to avoid these singularities.

To support this hypothesis we consider the case of a separated boundary layer, calculated as the limit of a transient development, when time becomes infinite. To simplify, we analyze the case of a theoretical flow in a unidimensional diffuser (Fig. 26).
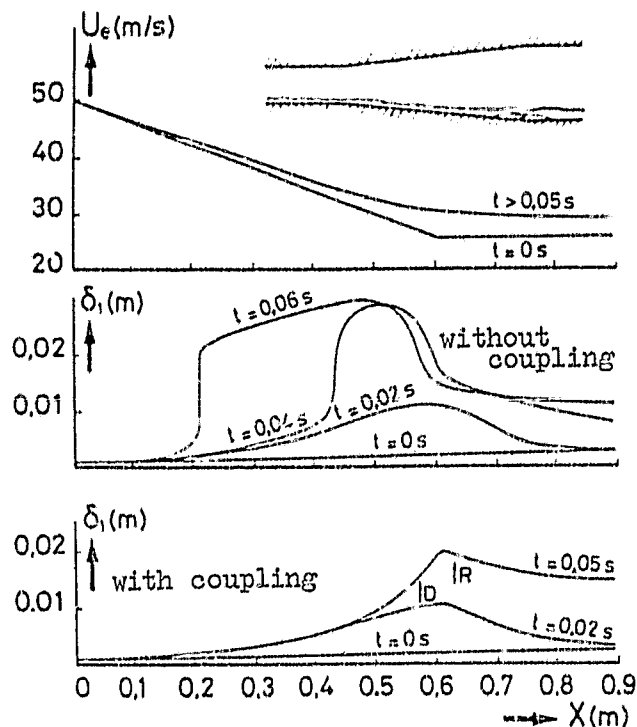

Fig. 26. Calculation of stationary boundary layer with recirculation airhole by unsteady method with coupling to external flow taken into account.

For t<0, the external velocity if constant, and the boundary layer obeys the stationary rules. At t= 0, the velocity is modified discontinuously. U_e decreases linearly in the $0 \leqslant x \leqslant 0.6$ range, and U_e is constant for x>0.6. For t>0, two calculations have been carried out. In the first, without coupling, the forced velocity at t=0 is maintained independent of time. Then, when t increases, a discontinuity in the evolution of δ_1 is found, which corresponds to the formation of a shock front.

In the second calculation, an attempt at coupling between the boundary layer and the nonviscous fluid was made, simply by using a unidimensional section principle

$$\frac{\partial}{\partial t}(S - 2\delta_1) + \frac{\partial}{\partial x} U_e(S - 2\delta_1) = 0 \qquad (51)$$

where S(x) is the diffuser cross section such that, at time t=0, the velocity distribution satisfies $U_e(S-2\delta_1)$=Cte.

In the second calculation, therefore, the velocity distribution develops as a function of time, according to Eq. (51). Under these

43

conditions, a perfectly stable stationary solution results. It is of interest to note that this solution includes a return flow offset, and that it shows no sign of singularities at points $C_f=0$. We stress the fact that this could only be obtained, by means of coupling between the nonviscous fluid and the boundary layer.

We point out that Nash and Scruggs have carried out turbulent boundary layer calculations, by using a transport equation model. In the theoretical examples with which they deal, they also observe the formation of singularities, if the external velocity is forced. By using a pressure gradient reduction procedure when the thickening of the boundary layer is too great, they show that the singularity can be avoided by maintaining a zone with return flow.

We also point out that Briley and McDonald have proposed a boundary layer calculation technique with a breakaway offset, by an unsteady method, while taking account of coupling with the nonviscous fluid.

4. Conclusions

Recent experiments and those which are underway are providing indispensable data on the behavior of oscillating turbulent boundary layers, which have been missing so far, and they can be the basis for deciding the validity of the calculation methods.

Meanwhile, some areas still remain partly unexplored. In the quite moderate Strouhal range (S<5), the effect on the viscous underlying layer of unsteadiness must be better defined. This problem perhaps is not too crucial for Strouhal numbers, since the proposed methods of calculation give results which, as a whole, are quite consistent with each other and with those of experiments, at least when the average pressure gradient is zero. For higher Strouhal numbers (on the order of 20), the problem is much greater. Actually, unsteady perturbations show up in a layer, the thickness of which decreases when the Strouhal number increases and can be limited to the thickness of the underlying layer. Therefore, it is thought that prediction of the coefficient of friction and of its amplitude and phase depends mainly on good modeling of the turbulence in

44

the underlying layer. Under such conditions, a second problem is raised:
for these Strouhal numbers and the customary Reynolds number, the fre-
quency imposed on the flow, within the range of characteristic frequencies
of the turbulence. Interaction between the harmonic perturbation and
turbulence can then exist.

Breakaway and the formation of singularities in the boundary layer
calculation remain unsolved problems, even in laminar flow. Several
numerical studies, in laminar, as well as turbulent flow, have shown that
singularities can develop inside the boundary layer, but interpretation
and theoretical study of them are incomplete. These singularities fre-
quently appear to clearly oppose the validity of the hypotheses used to
establish the boundary layer equations. Nevertheless, it can be hoped
to remove these difficulties in a number of cases, by turning to coupling
with the external flow.

REFERENCES

1. Acharya, M., "Measurements and predictions of a fully developed turbulent channel flow with imposed controlled oscillations," Stanford University, Ph.D., 1975.

2. Arnal, D., J. Cousteix, R. Michel, "Boundary layer developing with positive pressure gradient in an external turbulent flow," ONERA, La Recherche Aerospatiale No. 1976-1.

3. Binder, G., M. Garnier, J.L. Kueny, R. Laty, "Unsteady turbulent boundary layers," Institute of Mechanics, Scientific and Medical University of Grenoble, May 1977.

4. Bradshaw, P., "Calculation of boundary layer development using the turbulent energy equation," NPL Aero Report 1288, Feb. 1969.

5. Briley, W.R., H. McDonald, "Numerical prediction of incompressible separation bubbles," J. Fluid Mech. 69, part 4, 631-656 (1975).

6. Carr, L.W., "Standardization of computational experiments in unsteady turbulent boundary layer flow," NASA TM-78445, Dec. 1977.

7. Cebeci, T., L.W. Carr, "A computer program for calculating laminar and turbulent boundary layers for two-dimensional time-dependent flows," NASA TM-78470, March 1978.

8. Charnay, G., G. Comte-Bellot, J. Mathieu, "Development of a turbulent boundary layer on a flat plate in an external turbulent flow," AGARD-CP-93, 1971.

9. Charnay, G., M.P. Melinand, "Study of the structure of turbulent boundary layers which develop in the presence of a pulsed external flow," Contract DRME 72 1774, Fluid Mechanics Laboratory, Central School of Lyon, 1975.

10. Cousteix, J. and R. Houdeville (ed) (a), Report to Eurovisc working group meeting, "Unsteady turbulent boundary layers and shear flows," ONERA-CERT, Toulouse, 10-11 January 1977.

11. Cousteix, J., A. Desopper, R. Houdeville (b), "Structure and development of a turbulent boundary layer in an oscillatory external flow," Symposium on Turbulent Shear Flows, Pennsylvania, April 1977.

12. Cousteix, J., R. Houdeville, A. Desopper (c), "Experimental results and methods of calculation of turbulent boundary layers in unsteady flow," AGARD-CP-227, Ottawa, September 1977.

13. Cousteix, J., R. Houdeville (d), "Turbulent boundary layer calculations in unsteady flow. Numerical methods in applied fluid dynamics," University of Reading, 4-6 January 1978.

14. Cousteix, J., R. Houdeville (e), " Syntheses of studies carried out on turbulent boundary layers in unsteady flow," R.T. OA No. 29/2259, May 1978.

15. Cousteix, J., R. Houdeville (f), "First results of study of turbulent boundary layers in pulsed flow with average pressure gradient," 15th Colloquium on Applied Aerodynamics, Marseille, 7-9 November 1978.

16. Eichelbrenner, E.A. (ed), "Recent research on unsteady boundary layers," IUTAM, Symposium 1971, Quebec.

17. Farn, C.L.S., V.S. Arpaci, J. Clark, "A finite difference method for computing unsteady, incompressible, laminar boundary layer flows," U.S. Aerosp. Res. Lab. Rept. ARL 66-0010, Part III (1966).

18. Green, J.E., "Application of Head's entrainment method to the prediction of turbulent boundary layers and wakes in compressible flow," RA E, Technical Report 72079, 1972.

19. Hill, P.G., A.H. Stenning, "Laminar boundary layers in oscillatory flow," Trans. ASME Series D 82, 593 (1960).

20. Houdeville, R., A. Desopper, J. Cousteix, "Experimental analysis of average and turbulent characteristics of an oscillatory boundary layer. Attempts of theoretical prediction," Euromech 73, Aix-En-Provence 13-15 April 1976. ONERA TP No. 1976-30 (see also la Rech. Aerosp. no. 1976-4).

21. Jonsson, I.G., "A new approach to oscillatory rough turbulent boundary layers," Institute of Hydrodynamics and Hydraulic Engineering. Technical University of Denmark. ISVA Series Paper No. 17, Lingby, 1978.

22. Jonsson, I.G., N.A. Carlsen, "Experimental and theoretical investigations in an oscillatory turbulent boundary layer," Journal of Hydraulic Research 14/1, 45-60 (1976).

23. Karlsson, S.K.F., "An unsteady turbulent boundary layer," Journal of Fluid Mech. 5, 622-636 (1959).

24. Kenison, R.C., "An experimental study of the effect of oscillatory flow on the separation region in a turbulent boundary layer," AGARD-CP-227, Ottawa, 1977.

25. Kuhn, G.D., J.N. Nielsen, "Studies of an integral method for calculating time-dependent turbulent boundary layers," Project SQUID, Technical Report NEAR-2-PU, October 1973.

26. Mainardi, H., P.K. Panday, R. Barriol, "Pulsed turbulent flow in conduits," 14th Colloquium on Applied Aerodynamics, Toulouse 7-9 November 1977.

27. Marshall, F.J. (ed), "Fluid dynamics of unsteady, three dimensional and separated flows," Project SQUID, Workshop Georgia Inst. of Techn., 10-11 June 1971.

28. McCroskey, W.J., "Some current research in unsteady fluid dynamics. The 1976 Freeman Scholar lecture." Journal of Fluids Engineering 99, (March 1977).

29. McCroskey, W.J., J.J. Philippe, "Unsteady viscous flow on oscillating airfoils," ONERA, T.P. No. 1362, (1974).

30. McDonald, H., S.J. Shamroth, "An analysis and application of the time dependent turbulent boundary layer equations," AIAA Journal 9/8, (Aug. 1971).

31. Michel, R., C. Quemard, R. Durant, "Application of mixing length scheme to study of equilibrium turbulent boundary layers," ONERA N.T. No. 154, 1969.

32. Nash, J.F., R.M. Scruggs, "Unsteady boundary layers with reversal and separation," AGARD-CP-227, Ottawa, 1977.

33. Patel, M.H. (a), "On laminar boundary layers in oscillatory flow," Proc. R. Soc. Lond. A. 347, 99-123 (1975).

34. Patel, M.H. (b), "On turbulent boundary layers in oscillatory flow," Proc. R. Soc. Lond. A. 353, 121-144 (1977).

35. Patel, M.H. (c), "Two simplified integral approaches to the oscillating turbulent boundary layer," Communication presented to EUROVISC working group meeting, Orleans, February 1978.

36. Patel, M.H. (d), "The oscillating turbulent boundary layer: Experimental data," private communication.

37. Riley, N., "Unsteady laminar boundary layers," SIAM Review 17/2, (April 1975).

38. Schachenmann, A.A., D.O. Rockwell, "Oscillating turbulent flow in a conical diffuser," Journal of Fluids Engineering, 695-701 (December 1976).

39. Sears, W.R., D.P. Telionis, "Boundary layer separation in unsteady flow," SIAM J. Appl. Math. 28/1, (January 1975).

40. Shen, S.F., J.P. Nenni, "Asymptotic solution of the unsteady two-dimensional incompressible boundary layer and its implication on separation," Symposium on Unsteady Aerodynamics, R.B. Kinney (ed.), pp. 245-259, 1975.

41. Simpson, R.L., "Features of unsteady turbulent boundary layers as revealed from experiments," AGARD-CP-227, Ottawa, 1977.

42. Singleton, R.E., J.F. Nash, L.W. Carr, V.C. Patel, "Unsteady turbulent boundary layer analysis," NASA TM X-62, 242 (February 1973).

43. Stuart, J.T., "Double boundary layers in oscillatory viscous flow," Journal of Fl. Mech. 24, Part 4, (April 1966).

44. Stuart, J.T., "Unsteady boundary layers," Recentes recherches sur les couches limites instationnaires [Recent Research on Unsteady Boundary Layers], E.A. Eichelbrenner (ed.), Symposium IUTAM, 1971.

48

45. Telionis, D.P. (a), "Calculations of time-dependent boundary layers," Unsteady Aerodynamics, Vol. I, R.B. Kinney (ed.), pp. 155-190, July 1975.

46. Telionis, D.P. (b), "On the dynamics of eddy viscosity models for turbulent boundary layers," Archives of Mechanics Warsaw 28/5-6, 997-1010 (1976).

47. Telionis, D.P. (c), "Unsteady boundary layers, separated attached," AGARD-CP-227, Ottawa 26-28 September 1977.

48. Telionis, D.P., M.S. Romaniuk, "Velocity and temperature streaming in oscillating boundary layers," AIAA Journal 16/5, (May 1978).

49. Williams, J.C. III, W.D. Johnson, "New solutions to the unsteady laminar boundary layer equations including the approach to unsteady separation," AIAA Journal 12/10, (October 1974).